CHALMERS
UNIVERSITY OF TECHNOLOGY

Reverse assistance steering control for long combination vehicles

Master's thesis in Mobility Engineering

Pavan Kumar Adiga Nagaraj
Niveditha Krishnakumar

DEPARTMENT OF MECHANICS AND MARITIME SCIENCES

CHALMERS UNIVERSITY OF TECHNOLOGY
Gothenburg, Sweden 2025
www.chalmers.se

Master's Thesis in Mobility Engineering

Reverse Assist Steering Control for Long Combination Vehicles

Pavan Kumar Adiga Nagaraj
Niveditha Krishnakumar

CHALMERS
UNIVERSITY OF TECHNOLOGY

Department of Mechanics and Maritime Sciences
Division of Vehicle Engineering and Autonomous Systems
Chalmers University of Technology
Gothenburg, Sweden 2025

Reverse assistance steering control for long combination vehicles

Supervisor:
Mukesh Choudhary, Volvo Group Trucks Technology
Zhaohui Ge, Vehicle Dynamics group, Mechanics & Maritime Sciences, Chalmers

Examiner:
Bengt Jacobson, Vehicle Dynamics group, Mechanics & Maritime Sciences, Chalmers

Master's Thesis 2025
Department of Mechanics and Maritime Sciences
Chalmers University of Technology
SE-412 96 Gothenburg
Sweden
Telephone +46 31 772 1000

Reverse assistance steering control for long combination vehicles

Pavan Kumar Adiga Nagaraj
Niveditha Krishnakumar
Department of Mechanics and Maritime Sciences
Division of Vehicle engineering and autonomous systems, Vehicle Dynamics group
Chalmers University of Technology

Abstract

Greenhouse gas emissions are a global concern, with the transportation sector being a significant contributor. Enhancing energy efficiency in transportation can play a crucial role in mitigating these emissions. One promising approach to achieving this is the introduction of long combination vehicles (LCVs), which improve logistical efficiency by increasing load-carrying capacity. By reducing the number of vehicles needed to transport the same amount of cargo as a single-combination vehicle, LCVs help lower emissions and promote more sustainable transportation.

However, LCVs also present substantial challenges for drivers. Their increased length and weight reduce maneuverability in tight spaces and pose stability concerns at higher speeds. This can, to a large extent, be handled by legislation based on performance-based standards (PBS) [1], but reversing is not covered in today's PBS. The vehicle becomes more unstable as the number of articulation joints increases, as a result blind spots are created, limited visibility, and the need for precise articulation control. In certain situations, where the turning radius is restricted, drivers may be required to decouple and reposition trailers to complete a reversing maneuver. Additionally, most trucks lack onboard visualization systems to assist drivers during these operations.

This research explores an innovative solution by utilizing optimally controlled, multiple steered axles in LCVs. By actively managing the articulation angles, this approach aims to address maneuverability challenges, improve stability, and enhance overall vehicle performance. The primary focus of this thesis is to develop and implement a reverse steering assist system with a control strategy for the articulation angles of LCVs during reversing maneuvers. We specifically utilize an A-double combination vehicle, equipped with two steerable axles—one on the tractor and one on the last axle of the final trailer. This solution improve the maneuverability of the combination vehicle, ultimately enhancing operational efficiency and safety.

Keywords: Long combination vehicle, Reversing, Steering assist, Articulation angle control.

Acknowledgements

We would like to extend our heartfelt gratitude to our university supervisor, Zhaohui Ge, and our examiner, Bengt Jacobson. Their professional expertise and unwavering enthusiasm have been invaluable throughout our project.

We are also very grateful of the industrial supervisor from Volvo Group, Mukesh Choudhary, and our manager, Mats Lillieroth, for providing us with this incredible opportunity and challenge. Also, we would like to thank Parinaz Sedarati and Hans Westerlind for their support. Their encouraging environment and excellent facilities played a crucial role in the successful completion of our project.

In addition, we extend our gratitude to our operational test leader, Tommi Saarikoski, for providing valuable insights into the driving dynamics and challenges of the A-double combination. His guidance was instrumental in setting up the demonstration test.

Additionally, we express our sincere appreciation to our senior, Shreekara Ramesh, for his support and guidance. We are also deeply grateful to our beloved friends and parents for their unwavering support and companionship. Their encouragement gave us the confidence to embrace the unknown and overcome challenges, even in the most difficult moments.

Pavan Kumar Adiga Nagaraj, Niveditha Krishnakumar , Gothenburg, October 2025

List of Acronyms

ARC	Active Reverse Control
CAARP	Controllable Articulated Angle-oriented Reverse Principle
CAN	Controller Area Network
CARE	Continuous-time Algebraic Riccati equation
ECU	Electromic Control Unti
GTT	Group Truck Technology
HCT	High Capacity Transport
HMI	Human Machine Interface
KPI	Key Performance Indicator
LAARP	Locked Articulation Angle-oriented Reverse Principle
LCV	Long Combination vehicle
LQR	Linear Quadratic Regulator
LSOT	Low Speed Off Tracking
LSSP	Low Speed Swept Path
MPC	Model Predictive Control
OEM	Original equipment manufacturer
PBS	Performance-based Standards
PI	Proportional Intergral
PPC	Pure Pursuit Controller
RC	Remote Control
SSCL	Steady-state Circling Limitation
TSC	Total Steering Correction
TSW	Transient Swept Width
VSA	Virtual Steering Angle
VTM	Volvo Transport Models

Nomenclature

Below is the nomenclature of indices, sets, parameters, and variables that have been used throughout this thesis.

Indices

i	Vehicle unit number
j	Axle number

Parameters

For Kinematic vehicle model

L_1	Tractor wheel base [m]
b_1	Distance from pivot 1 to tractor rear axle [m]
L_2	Distance from pivot 1 to rear axle of semi-trailer-1 [m]
b_2	Distance from rear axle of semi-trailer-1 to pivot 2 [m]
L_3	Distance from pivot 2 to axle of dolly [m]
b_3	Distance from dolly axle to pivot 3 [m]
L_4	Distance from pivot 3 to rear axle of semi-trailer-2 [m]

For All axle vehicle model

L_{12}	Tractor front axle to first axle of rear axle group [m]
L_{13}	Tractor front axle to last axle of rear axle group [m]
b_1	Distance from pivot 1 to tractor last axle of rear axle group [m]
L_{21}	Distance from pivot 1 to first axle in rear axle group of semi-trailer-1 [m]
L_{22}	Distance from pivot 1 to second axle in rear axle group of semi-trailer-1 [m]

L_{23}	Distance from pivot 1 to third axle in rear axle group of semi-trailer-1 [m]
b_2	Distance from third axle in rear axle group of semi-trailer-1 to pivot 2 [m]
L_{31}	Distance from pivot 2 to first axle of dolly [m]
L_{32}	Distance from pivot 2 to rear axle of dolly [m]
b_3	Distance from dolly rear axle to pivot 3 [m]
L_{41}	Distance from pivot 3 to first axle in rear axle group of semi-trailer-2 [m]
L_{42}	Distance from pivot 3 to second axle in rear axle group of semi-trailer-2 [m]
L_{43}	Distance from pivot 3 to third axle in rear axle group of semi-trailer-2 [m]

Variables

δ_{11}	Steering angle of the tractor [rad]
δ_{41}	Steering angle of the semi-trailer-2 [rad]
v_{1x}	Longitudinal velocity of the tractor [m/s]
ϕ_1	Yaw angle of the tractor [rad]
$\dot{\phi}_1$	Yaw rate of the tractor [rad/s]
ϕ_2	Yaw angle of the semi-trailer-1 [rad]
$\dot{\phi}_2$	Yaw rate of the semi-trailer-1 [rad/s]
ϕ_3	Yaw angle of the dolly [rad/s]
$\dot{\phi}_3$	Yaw rate of the dolly [rad/s]
ϕ_4	Yaw angle of the semi-trailer-2 [rad/s]
$\dot{\phi}_4$	Yaw rate of the semi-trailer-2 [rad/s]
θ_1	Articulation angle between the tractor and the semi-trailer-1 [rad/s]
θ_2	Articulation angle between the semi-trailer-1 and the dolly [rad/s]
θ_3	Articulation angle between the dolly and the semi-trailer-2 [rad/s]
$\dot{\theta}_1$	Articulation angle rate between the tractor and the semi-trailer-1 [rad/s]
$\dot{\theta}_2$	Articulation angle rate between the semi-trailer-1 and the dolly [rad/s]
$\dot{\theta}_3$	Articulation angle rate between the dolly and the semi-trailer-2 [rad/s]

$\dot{\theta}_3$	Articulation angle between the dolly and the semi-trailer-2 [rad/s]
X_{11}	X coordinate of the front axle of the tractor [m]
Y_{11}	Y coordinate of the front axle of the tractor [m]
X_{12}	X coordinate of the lumped rear axle of the tractor [m]
Y_{12}	Y coordinate of the lumped rear axle of the tractor [m]
X_{21}	X coordinate of the lumped axle of the semi-trailer-1 [m]
Y_{21}	Y coordinate of the lumped axle of the semi-trailer-1 [m]
X_{31}	X coordinate of the lumped axle of the dolly [m]
Y_{31}	Y coordinate of the lumped axle of the dolly [m]
X_{41}	X coordinate of the lumped axle of the semi-trailer-2 [m]
Y_{41}	Y coordinate of the lumped axle of the semi-trailer-2 [m]
X_{p1}	X coordinate of the rear coupling point on the tractor unit [m]
Y_{p1}	Y coordinate of the rear coupling point on the tractor unit [m]
X_{p2}	X coordinate of the rear coupling point on the semi-trailer-1 unit [m]
Y_{p2}	Y coordinate of the rear coupling point on the semi-trailer-1 unit [m]
X_{p3}	X coordinate of the rear coupling point on the dolly unit [m]
Y_{p3}	Y coordinate of the rear coupling point on the dolly unit [m]

Contents

List of Figures

List of Tables

1
Introduction

In this chapter, background information, research questions, assumptions, and a review of literature that outlines the related work carried out in this field of study are presented.

1.1 Background

The transportation of goods is a fundamental component of any economy. In particular, land-based freight transport is predominantly carried out by trucks. According to Eurostat data from 2022, road transport in the European Union accounted for approximately 24.9% of the total freight transport performance, measured in tonne-kilometers. This represents a notable increase from 2012, when the share was approximately 22% [2].

Furthermore, in 2023, new truck registrations in the European Union rose significantly by 16.3%, reaching a total of 327,896 units. This growth was largely driven by an 8.5% increase in the sales of medium and heavy commercial vehicles, which amounted to approximately 94,800 units [3].

In the Nordic countries, there has been a progressive shift towards permitting the use of Long Combination Vehicles (LCVs). Finland was the first among these countries to legalize LCVs specifically A-double and AB-double combination in 2019. Subsequently, in December 2023, Sweden officially legalized the operation of LCVs with a total length of up to 34.5 meters. The initial field trials in Sweden began as early as 2009. The first official High Capacity Transport (HCT) combination introduced was a 90-tonne truck and B-double timber configuration. Additional field tests commenced in February 2012 for the transportation of general cargo between Gothenburg and Malmö. These included a 66-tonne double center-axle trailer combination (DUO-CAT) and an 80-tonne A-double combination (DUO-Trailer) [4].

In Sweden, two of the most common configurations for long-distance freight transport are the B-double combination and the Nordic combination. These vehicle types can reach a total length of up to 25.25 meters, enabling the efficient transport of large volumes of goods over extended distances. Recently, there has been a growing trend toward the legalization and adoption of even longer vehicle combinations across the region.

Key Technical Requirements and Legal Provisions:
According to regulation TSFS 2025:17 [5], the following conditions apply to vehicle combinations exceeding 25.25 meters and up to a maximum of 34.5 meters in total length:

This new regulation is applicable only on approved roadways, as designated under Sweden's Traffic Ordinance. It will enter into force on 15 April 2025, superseding the previous regulation, TSFS 2023:42 [6].

The five approved vehicle configurations [7] are as follows:

- **A-double:** Tractor unit + semi-trailer + dolly + second semi-trailer
- **AB-double:** Rigid truck + dolly + link semi-trailer + semi-trailer
- **B-double:** Tractor unit + link semi-trailer + semi-trailer (link trailer length $\leq 12\,\mathrm{m}$)
- **C-double:** Rigid truck + two drawbar trailers (maximum height: 4.0 m)
- **Nordic combination:** Rigid truck + dolly + semi-trailer (approximate total length: 27 m)

The increasing deployment of heavy-duty trucks and innovative vehicle configurations underscores the rising demand for efficient and cost-effective transportation solutions in Europe, particularly in regions where road transport plays a pivotal role in the logistics sector.

The major players in the truck manufacturing industry, such as Daimler, Volvo Group and Scania AB, mainly focuses on the truck manufacturing and are not typically involved in the trailer manufacturing business. There remains a distinct separation between truck and trailer manufacturers, with each segment operated by different companies. While truck Original equipment manufacturer (OEM) are dedicated to the design and production of the vehicle's cab and drivetrain, the responsibility for trailers falls to specialized companies, such as Wabash, Utility, and Schmitz Cargobull, among others.

This division has created a gap in the integration of technologies between the truck and trailer sectors. However, recent developments indicate a growing effort to bridge this gap, as trailer manufacturers are increasingly incorporating advanced technologies aimed at enhancing the efficiency and sustainability of trailers. Innovations in telematics, communication systems, and fuel-saving technologies are being integrated into trailer designs. For these technologies to deliver optimal performance, effective integration with existing truck systems is essential. The communication signal specifications relevant to this integration are defined in ISO 11992-3 [8]. OEMs are advocating for the inclusion of additional communication signals to support a wider range of trailer functions within truck control systems.

Recognizing the need for improved integration, truck OEMs are increasingly collaborating with trailer manufacturers to explore more efficient solutions that incorporate advanced communication protocols and technologies. This collaboration aims to develop fully integrated systems in which tractor and trailer operate seamlessly, thus

improving fuel efficiency, sustainability, and overall cost-effectiveness in transportation operations.

The current trend points toward a more integrated approach in the design and development of both trucks and trailers, with an emphasis on creating connected, intelligent vehicles that are not only economically viable but also environmentally sustainable. This collaboration between truck and trailer manufacturers is a step toward addressing the growing demand for smart logistics solutions, which is becoming increasingly important as the industry seeks to meet stricter environmental regulations and improve operational efficiency.

This integration is expected to play a key role in the future of transportation, with an increasing focus on digital technologies, telematics, and automation, helping to provide more efficient, connected, and environmentally friendly fleets.

In the trucking industry, the trailers that are predominantly used do not have steering axle, instead it relies only on the tractor steering. Existing technologies like "Trailer Assist," commonly used in passenger vehicles, have greatly improved the ease of reversing vehicles with trailers attached. This technology typically utilizes cameras that provide a clear view from the rear of the vehicle, covering blind spots and making it easier for drivers to reverse safely. The majority of passenger car manufacturers have integrated this system into their vehicles, enhancing convenience and safety [9].

However, similar technologies are not yet widely available for heavy trucks and long combinations, creating significant challenges for drivers when reversing. In the case of long combinations, such as the A-double combination which includes a tractor, semi-trailer, dolly, and a second semi-trailer reversing becomes particularly difficult. This is due to the complexity introduced by the varying lengths of each unit, especially the dolly, which is the most sensitive and challenging part to maneuver when reversing. The driver must navigate the changing articulation angles between the different units, further complicating the task.

Trailer manufacturers are beginning to address this issue by developing advanced reversing assist systems designed specifically for trucks and long combinations. For instance, companies like ZF have introduced an advanced "Reverse Assistance" function that utilizes a rearward-directed camera on (last) trailer end with a 180-degree view to provide the driver with comprehensive feedback during reversing. This system improves visibility and helps the driver navigate tight spaces more safely [10].

Similarly, Bosch has developed a reversing assist technology that employs a rear-mounted camera on the first vehicle unit to detect and continuously measure the articulation angle to measure the coupling angles of the units in a combination vehicle. These sensors, along with a Human-Machine Interface (HMI), provide real-time data to the driver, helping them understand the position and movement of the vehicle as they reverse. The technology is designed to ensure better control over the vehicle during reversing, reducing the risk of accidents or collisions [11].

These developments highlight the growing need for integrating advanced technologies into the truck and trailer sector. As the logistics industry continues to evolve, such systems will play a vital role in enhancing driver safety, improving efficiency, and reducing the complexity of handling large, articulated vehicles. By addressing the unique challenges of reversing long combinations, manufacturers can significantly improve the overall driving experience.

The tractor-semitrailer combination, which has a single articulation angle and is comparatively easier to operate due to its more predictable movement, already includes reverse assistance solutions. However, an LCV that has multiple articulation angles has significantly increased complexity when it comes to reversing and this have limited the availability of comparable assistance solutions.

1.2 Purpose

The purpose of this thesis is to investigate the benefits of incorporating a actively steered axle on a semi-trailer in combination with the steering axle of the tractor unit. The lateral characteristics of interest include the low speed swept path (LSSP) at low speeds, particularly during reverse maneuvers. The primary objective of this work is to develop a low-speed reverse assistance functionality for an A-double combination.

LCVs, such as the A-double configuration, which is solely based on the steering and propulsion of the tractor unit, often face significant challenges when maneuvering in confined spaces. By introducing an additional active steering system on the last axle of the second trailer of an A-double combination, these maneuverability challenges, especially during reversing, can be mitigated At low forward speeds, a self-steering axle (also known as a friction-steered or swiveling axle) is often sufficient to improve cornering. However, during reversing, the axle must be actively steered, meaning it should follow a commanded steering angle, in order to maintain control and enhance overall maneuverability.

1.3 Goals

The aim of this thesis is to,

1. Investigate the existing market solutions available for the low-speed reversing.

2. Understanding the difficulties faced by the driver while reversing the LCV.

3. Develop a controller utilizing two steerable axles (one on the tractor front axle and one on the last semi-trailer last axle).

4. Test the controller and compare the effects of having laden/unladen mass on the last trailer while reversing in Volvo Transport Model (VTM).

5. Setup the controller model setup for a real vehicle.

6. Implement the concept in a test vehicle with a control knob and a HMI display to provide real-time feedback to the driver.

1.4 Assumptions

The following assumptions hold as a base for this thesis.

1. The reversing maneuver will be driven at low speeds (< 8 km/h).

2. The path in which the vehicle will have to travel will be set by the driver with a control knob as the driver plays an important role in the path planning, Hence the path planners will not be designed in this thesis. The visual feedback is provided based on the real time measurement of articulation angle sensor data instead of camera feed.

3. An articulation angle sensor is available at each articulation point of the A-double combination.

1.5 Limitations

The limitations of this thesis are as follows.

1. The vehicle setup is limited to an A-double which comprises a 6×4 tractor with a steerable front axle, a three-axle semi-trailer, a two axle dolly unit and a three axle semi-trailer with the last axle being a steerable axle.

2. The vehicle is considered to be driven only on a flat surface.

3. Steering-rate limiters were not considered in this thesis.

1.6 Literature Review

The long combination vehicle (LCV) typically consists of multiple units that are combined into a configuration to carry out the commercial transport activity. The major challenge with articulated vehicles is to reverse them which requires a skilled driver. Previous publication work done on A-double combination reverse is being discussed in the subsection (1.6).

In the study by Ashok et al. [12], the reverse assist for an A-double combination vehicle was implemented, wherein only the front axle of the tractor is the steerable axle. The equations of motion were formulated using a kinematic modelling

approach, and two different control strategies were discussed: one being the Path Prediction Controller (PPC) and the other a Radius controller. The study was conducted both in a simulation environment and with a scaled Remote-Control (RC) vehicle.

Matsushita et al. [13] studied three control strategies for a double trailer vehicle. The first is a velocity controller, and the second has different types of steering controller. The velocity controller proposed in this research can be used regardless of the number of connected trailer units. In the first steering controller, the vehicle could reverse but the tractor unit was unstable. To overcome this, a second steering controller was proposed that used the Lyapunov function and backstepping.

According to a study conducted by Morales et al. [14] for multi-trailer combination trucks, the suggested system could prevent Jack-knifing and inter-unit collisions. The steering-wheel feedback force has been adjusted based on the curvature limit calculated for a specific combination of one or more trailers, implements jackknife avoidance. Steering limitations have been introduced to the last trailer unit wherein it has been considered as a virtual tractor to avoid jack-knifing and inter-unit collision.

Rimmer et al. [15] in her work on a reverse control technique implemented two controllers for a B-double combination vehicle. The first one being a preview point controller and the second one is a state feedback controller with Linear Quadratic Regulator (LQR) tuning in which the later outperforms. While reversing an articulated, there will be some delay, which is compensated by considering the lateral offset point in Preview point controller and in State feedback controller it is computed by using the look ahead distance. The articulation angles were measured using an articulation angle sensor.

The study conducted by Ge et al. [16] investigates a reversing strategy that addresses the limitations associated with Steady-state Circling Limitation (SSCL). The author propose two novel reversing principles based on articulation angles, derived through a kinematic model. The first principle, the Controllable Articulated Angle-oriented Reverse Principle (CAARP), primarily aims to prevent inter-unit collisions. The second principle, the Locked Articulation Angle-oriented Reverse Principle (LAARP), is employed in scenarios where the application of CAARP is not feasible.

Oskar et al. [17] have pursued a cascaded control approach, where the low-level controller is a state feedback controller stabilizing the articulation angles, and the high-level controller implements path planning and control (PPC) to account for path tracking.

Astolfi et al. [18] have proposed nonlinear control laws utilizing Lyapunov techniques to design stabilizing controllers for path tracking of a two-body articulated vehicle. The proposed approach ensures stability for both forward and backward

motions along a straight line or circular path. The control variables include the longitudinal speed and the steering angle of the front axle of the tractor.

Altafini et al. [19] have studied a hybrid control scheme to stabilize the backward motion of a miniaturized truck and trailer system along simple paths. The approach employs a switching controller that alternates between forward and backward closed-loop control to prevent jackknifing.

Oskar et al. [20] have developed a path planning and path-following control solution designed to automatically plan and execute complex parking and obstacle avoidance maneuvers by combining both forward and backward motions. The approach utilizes a lattice-based path planning framework to ensure kinematic feasibility and collision-free paths. Additionally, a path controller is designed to regulate lateral and angular errors during path execution.

Sudhakaran et al. [21] have developed an inverse kinematic controller and an I/O linearization controller for a tractor-semi-trailer combination to control and stabilize the articulation angle. The controller ensures stable tracking of the tractor's reference path while reversing.

The limitations of existing studies by Ashok et al., Morales et al. and Oskar et al. [17] are that only the front axle of the tractor is steered, and visual feedback is provided to the driver on the HMI with a camera feed.

Trailer Steering:
Trailer steering systems are mainly categorized into two types: self-steered and actively steered. Under actively steered systems, there are hydraulic and electro-hydraulic (active) steering systems.

Self-steering (or tracking) axles employ lateral forces generated during cornering, transmitted through the kingpin geometry, to induce a slight steer angle of the wheels toward the inside of the turn. This mechanism improves vehicle stability and reduces tire scrub by aligning the axle more closely with the trajectory of the combination.

When operating in reverse, however, the self-steering axle must be either locked or lifted. If left active, the wheels will steer in the opposite direction to that required for the maneuver, resulting in adverse handling characteristics. This presents a particular challenge in confined reverse maneuvers, as the vehicle combination must first be driven forward to allow the steering system to self-center before the locking mechanism can be engaged.

Actively steered axles employ an electronic control system, in conjunction with hydraulic or electric actuators, to adjust the steering angle of the wheels in response to vehicle speed, articulation angle, and driver input. Unlike passive self-steering axles, which rely on lateral forces through the kingpin geometry, actively steered

axles receive direct commands from a control unit, allowing precise steering intervention to optimize vehicle dynamics.

During forward motion, active steering improves maneuverability at low speeds by reducing the turning radius, while enhancing stability at higher speeds through controlled counter-steer. When reversing, the system can maintain full steering functionality without the need for lifting or mechanical locking, as the steering response is governed by the control algorithm rather than passive geometry. This enables consistent and predictable axle behavior in confined spaces, eliminating the requirement to drive forward to centralize the wheels prior to a reversing maneuver.

In Europe, standard semi-trailers are commonly equipped with three rigid axles. Krone [22] has introduced a self-steered axle that operates similarly to the caster wheels on a shopping cart. The pivot points of the steering knuckles are located ahead of the axle center in the direction of travel. This configuration causes the axle to realign automatically when cornering in the forward direction. During reverse travel, the axle is locked by a brake cylinder. A stabilizing beam is incorporated to prevent uncontrolled movements of the steering knuckles during high-speed, straight-line travel.

The BPW self-steering axle [23] allows the wheels of the third axle to align naturally when navigating curves. The self-steering function ensures the wheels follow the turning radius, with undulating thrust plates sliding against each other to facilitate motion. The steering angle is set according to the load and is controlled purely mechanically. As with other self-steering systems, the axle is locked when reversing. A two-year study conducted by BPW demonstrated that more than 10,000 liters of fuel can be saved over a distance of 1 million kilometers. The same study showed that effective tractive forces are reduced by up to 60%, contributing to improved fuel efficiency and reduced tire wear.

BPW has also introduced an innovative electro-hydraulic auxiliary steering system known as Active Reverse Control (ARC) [24]. This system is specifically designed for the last axle of a semi-trailer. Traditionally, self-steering axles are locked during reversing, rendering them rigid. ARC overcomes this limitation by enabling fully automated steering during reverse maneuvers at speeds of up to 10 km/h. This improves maneuverability and reduces tire wear, even in confined or complex operating environments. Additionally, ARC can also be utilized during forward travel at low speeds, further enhancing agility. The result is reduced maneuvering time, lower maintenance costs, and increased operational efficiency.

The VSE Smart Steering System [25] is an advanced electronic steering solution designed to improve maneuverability and precision in multi-axle trailers, particularly for heavy-duty applications such as modular trailers, low-loaders, and wind turbine blade transporters. The Electronic Control Unit (ECU) determines the optimal steering angle for each axle and adjusts the wheel positions based on the sensor inputs. Designed to enhance maneuverability in confined spaces, the VSE Smart

Steering System is particularly well-suited for large multi-axle trailers that require precise steering, making it an ideal solution for urban and industrial environments.

Chiu et al. [26] have implemented a feed-forward & feedback control for the tractor-trailer combination. In the vehicle considered, the front axle of the tractor can be steered and the last axle of the trailer can be steered. The front axle steering input is given to the vehicle as a feed-forward control, where the steering input is provided by the driver, and a feedback control loop is implemented to provide control input to the rear axle steering of the trailer considering the stabilization of the hitch angle.

Odhams et al. conducted a study using actively steered trailers [27]. The vehicle that was considered in this study was a B-double. They devised a reversing algorithm that ultilizes path followers in which the steering angle of the first trailer will be controlled by the driver with a joystick. The steering angle of the second trailer is then controlled by their reversing controller. The demand for the steering angle of the tractor was sent to the driver using the driver as a servo.

Werner et al. [28] have developed a path-tracking control which combines the LQR and output feedback approximation to maintain precision in path-tracking. Wang et al. [29], have presented an adaptive and robust nonlinear controller based on Model Predictive Control (MPC) aimed at improving path tracking for tracked vehicles with steerable trailers for agricultural applications. The author designed an adaptive max-min MPC method to handle uncertainties and disturbances.

In the study presented by Chiu et al. and Odhams et al. the steering of the first trailer is controlled by the driver. In the study presented in by Werner et al., they have devised a non-linear controller. The objective of the present research project is to develop mathematical models for the steered front axle of the tractor, the last steered axle of the last semitrailer, and to develop a simple linear controller for both the steering inputs. The feasibility of this approach is supported by the existence of trailer steering systems and the demonstrated capability of existing controllers to manage multi-input multi-output (MIMO) systems. These prerequisites provide a solid foundation for the proposed modeling and control strategy. Furthermore, the available kinematic data will be utilized to provide visual feedback.

2
Vehicle Dynamics

Developing a control logic for reverse assist steering in an A-double combination requires a thorough understanding of vehicle dynamics and control theory. It is crucial to account for the influence of system dynamics in achieving the desired control objectives. The kinematic modeling process adheres to the standard coordinate system used for vehicle frames, following the right-hand coordinate system defined in ISO-8855 [30].

Given that the primary focus is on the reversing maneuver of the A-double combination, the model excludes resistive forces such as aerodynamic drag and rolling resistance. Hence, the kinematic model is considered in this study and is limited to a single-track model with planar dynamics which only accounts in XY-plane. This approach simplifies the system using geometric relationships and velocity constraints.

2.1 Vehicle Configuration

The vehicle combination used in this study is an A-double represented in Fig. (2.1), which consists the following.

1. Tractor of 6 × 4 configuration with steerable front axle
2. Semi-trailer-1 with three non-steerable axles
3. Dolly with two non-steerable axles
4. Semi-trailer-2 with two non-steerable axles and a steerable last axle

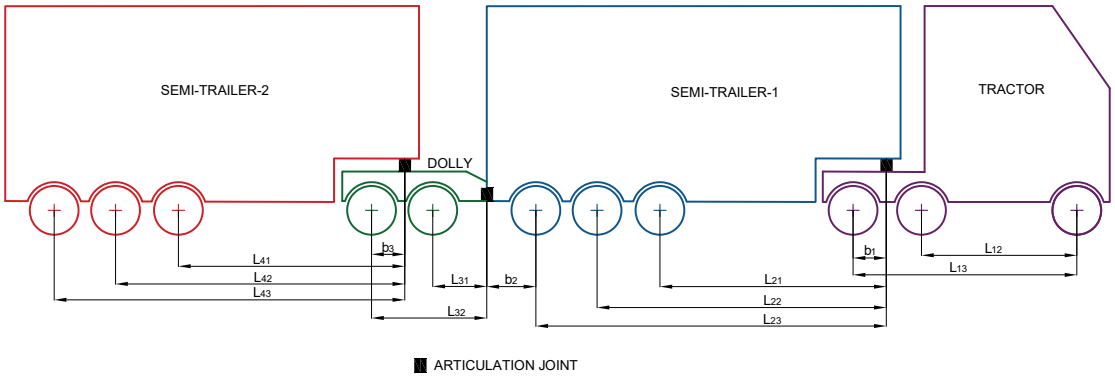

Figure 2.1: A-double combination truck with all the axles

The dimensions of A-double combination truck with all axles are shown in Table (2.1).

Table 2.1: Real vehicle parameters

Parameter	Description	Value	Unit
L_{12}	Tractor front axle to first axle of rear axle group	2.40	m
L_{13}	Tractor front axle to last axle of rear axle group	3.70	m
b_1	Distance from pivot 1 to tractor last axle of rear axle group	0.58	m
L_{21}	Distance from pivot 1 to first axle in rear axle group of semi-trailer-1	6.80	m
L_{22}	Distance from pivot 1 to second axle in rear axle group of semi-trailer-1	8.10	m
L_{23}	Distance from pivot 1 to third axle in rear axle group of semi-trailer-1	9.40	m
b_2	Distance from third axle in rear axle group of semi-trailer-1 to pivot 2	1.10	m
L_{31}	Distance from pivot 2 to first axle of dolly	3.90	m
L_{32}	Distance from pivot 2 to rear axle of dolly	5.21	m
b_3	Distance from dolly rear axle to pivot 3	0.66	m
L_{41}	Distance from pivot 3 to first axle in rear axle group of semi-trailer-2	6.80	m
L_{42}	Distance from pivot 3 to second axle in rear axle group of semi-trailer-2	8.10	m
L_{43}	Distance from pivot 3 to third axle in rear axle group of semi-trailer-2	9.40	m

To enable a kinematic model the modeling is as shown in Fig.(2.2), each unit is represented using a lumped axle approach, which avoids scrubbing (a.k.a. lateral fighting) between axles and retains steer-ability. As a result, the vehicle model being analyzed comprises a total of five axles, of which two are steerable.

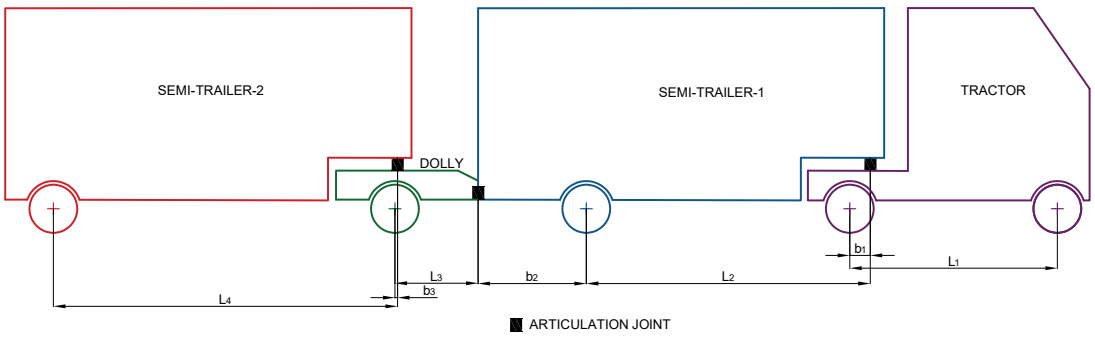

Figure 2.2: Lumped model of an A-double combination truck

The dimensions of the combination are presented in Table (2.2). Each trailer has a length of 40 feet, resulting in a total combination length of 32.5 meters. The track width for each axle is modelled as 2.5 meters.

Table 2.2: Kinematic vehicle model parameters

Parameter	**Description**	**Value**	**Unit**
L_1	Tractor wheel base	3.7	m
b_1	Distance from pivot 1 to tractor rear axle	0.58	m
L_2	Distance from pivot 1 to rear axle of trailer 1	8.10	m
b_2	Distance from rear axle of semi-trailer 1 to pivot 2	2.40	m
L_3	Distance from pivot 2 to axle of dolly	4.55	m
b_3	Distance from dolly axle to pivot 3	0.488	m
L_4	Distance from pivot 3 to rear axle of semi-trailer 2	9.40	m

2.1.1 Single-track kinematic model

The figure (2.3) represents a single-track kinematic model of an A-double combination vehicle.

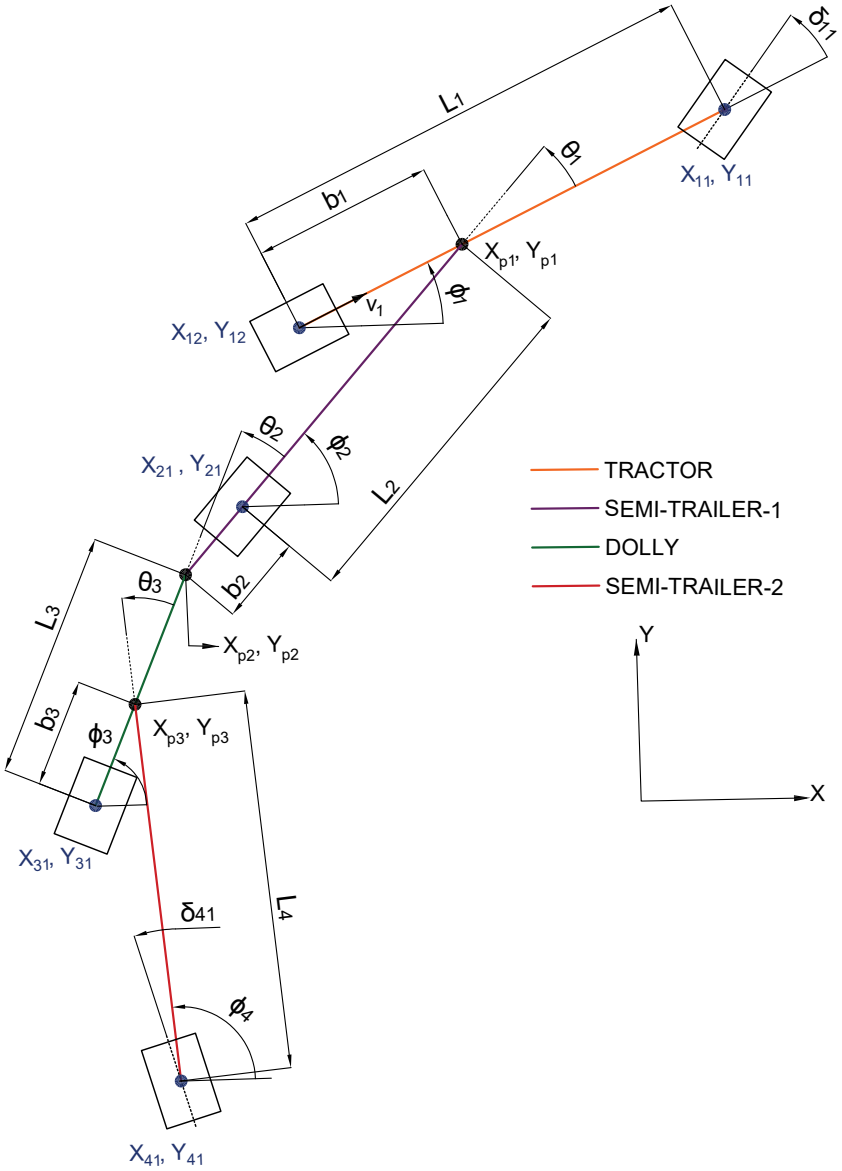

Figure 2.3: Kinematic model of an A-double

Using the kinematic constraints of the vehicle, the positions of the units are defined as follows.
The position of the front axle of the tractor is given by,

$$X_{11} = X_{12} + L_1 \cos(\phi_1) \tag{2.1}$$

$$Y_{11} = Y_{12} + L_1 \sin(\phi_1) \tag{2.2}$$

The position of the coupling point $p1$ is given by,

$$X_{p1} = X_{12} + b_1 \cos(\phi_1) \tag{2.3}$$

$$Y_{p1} = Y_{12} + b_1 \sin(\phi_1) \tag{2.4}$$

The position of the rear axle of the semi-trailer-1 is given by,

$$X_{21} = X_{p1} - L_2 \cos(\phi_2) \tag{2.5}$$

$$Y_{21} = Y_{p1} - L_2 \sin(\phi_2) \tag{2.6}$$

The position of the coupling point $p2$ is given by,

$$X_{p2} = X_{21} - b_2 \cos(\phi_2) \tag{2.7}$$

$$Y_{p2} = Y_{21} - b_2 \sin(\phi_2) \tag{2.8}$$

The position of the rear axle of the dolly is given by,

$$X_{31} = X_{p2} - L_3 \cos(\phi_3) \tag{2.9}$$

$$Y_{31} = Y_{p2} - L_3 \sin(\phi_3) \tag{2.10}$$

The position of the coupling point $p3$ is given by,

$$X_{p3} = X_{31} + b_3 \cos(\phi_3) \tag{2.11}$$

$$Y_{p3} = Y_{31} + b_3 \sin(\phi_3) \tag{2.12}$$

The position of the rear axle of the semi-trailer-2 is given by,

$$X_{41} = X_{p3} - L_4 \cos(\phi_4) \tag{2.13}$$

$$Y_{41} = Y_{p3} - L_4 \sin(\phi_4) \tag{2.14}$$

Differentiating the position equations with respect to time gives us the velocity at the points.
The velocity at the rear axle of the tractor is given by,

$$\dot{X}_{12} = v_1 \cos(\phi_1) \tag{2.15}$$

$$\dot{Y}_{12} = v_1 \sin(\phi_1) \tag{2.16}$$

The velocity at the tractor front axle is given by,

$$\dot{X}_{11} = \dot{X}_{12} - L_1 \sin(\phi_1)\dot{\phi}_1 \tag{2.17}$$

$$\dot{Y}_{11} = \dot{Y}_{12} + L_1 \cos(\phi_1)\dot{\phi}_1 \tag{2.18}$$

The velocity at point $p1$ is given by,

$$\dot{X}_{p1} = \dot{X}_{12} - b_1 \sin(\phi_1)\dot{\phi}_1 \tag{2.19}$$

$$\dot{Y}_{p1} = \dot{Y}_{12} + b_1 \cos(\phi_1)\dot{\phi}_1 \tag{2.20}$$

The velocity at the rear axle of semi-trailer-1 is given by,

$$\dot{X}_{21} = \dot{X}_{p1} + L_2 \sin(\phi_2)\dot{\phi}_2 \tag{2.21}$$

$$\dot{Y}_{21} = \dot{Y}_{p1} - L_2 \cos(\phi_2)\dot{\phi}_2 \tag{2.22}$$

The velocity at point $p2$ is given by,

$$\dot{X}_{p2} = \dot{X}_{21} + b_2 \sin(\phi_2)\dot{\phi}_2 \tag{2.23}$$

$$\dot{Y}_{p2} = \dot{Y}_{21} - b_2 \cos(\phi_2)\dot{\phi}_2 \tag{2.24}$$

The velocity at the rear axle of the dolly is given by,

$$\dot{X}_{31} = \dot{X}_{p2} + L_3 \sin(\phi_3)\dot{\phi}_3 \tag{2.25}$$

$$\dot{Y}_{31} = \dot{Y}_{p2} - L_3 \cos(\phi_3)\dot{\phi}_3 \tag{2.26}$$

The velocity at point $p3$ is given by,

$$\dot{X}_{p3} = \dot{X}_{31} - b_3 \sin(\phi_3)\dot{\phi}_3 \tag{2.27}$$

$$\dot{Y}_{p3} = \dot{Y}_{31} + b_3 \cos(\phi_3)\dot{\phi}_3 \tag{2.28}$$

The velocity at the rear axle of semi-trailer-2 is given by,

$$\dot{X}_{41} = \dot{X}_{p3} + L_4 \sin(\phi_4)\dot{\phi}_4 \tag{2.29}$$

$$\dot{Y}_{41} = \dot{Y}_{p3} - L_4 \cos(\phi_4)\dot{\phi}_4 \tag{2.30}$$

The articulation angle is defined as the difference between the yaw angles of the two consecutive units. The rate of change of articulation angles provide, articulation angle rate. Articulation angle and the articulation angle rate can be given as follows

$$\theta_i = \phi_i - \phi_{i+1} \tag{2.31}$$

$$\dot{\theta}_i = \dot{\phi}_i - \dot{\phi}_{i+1} \tag{2.32}$$

Where $i = 1, 2, 3$

In the lateral direction, the vehicle system satisfies non-holonomic constraints that limit motion perpendicular to the wheel plane. Equation (2.33) represents this limitation for a non-steered axle, ensuring that the lateral velocity component remains zero because of the no-slip condition.

$$\dot{X} \cdot \sin(\phi) - \dot{Y} \cdot \cos(\phi) = 0 \tag{2.33}$$

Each axle in the system is then given the general form. The non-holonomic restrictions implemented on the four axles are expressed by equations (2.34)–(2.37), which account for the steering angles (δ) and the respective yaw angles (ϕ) unique to each axle. In order to prevent lateral slip, these expressions specify the relationship between the velocities in the global X and Y directions.

$$\dot{X}_{11}\sin(\phi_1+\delta_{11})-\dot{Y}_{11}\cos(\phi_1+\delta_{11})=0 \tag{2.34}$$

$$\dot{X}_{21}\sin(\phi_2)-\dot{Y}_{21}\cos(\phi_2)=0 \tag{2.35}$$

$$\dot{X}_{31}\sin(\phi_3)-\dot{Y}_{31}\cos(\phi_3)=0 \tag{2.36}$$

$$\dot{X}_{41}\sin(\phi_4+\delta_{41})-\dot{Y}_{41}\cos(\phi_4+\delta_{41})=0 \tag{2.37}$$

Solving equations (2.34) - (2.37) gives the yaw rate for each unit. The articulation angle rates between vehicle units can then be calculated by substituting the yaw rate equation (2.32).

2.2 Vehicle Models Validation

The VTM [31], a high-fidelity vehicle model, is used to evaluate the equations produced from the kinematic single-track model in Section (2.1.1). A step steer maneuver was simulated with different vehicle speed to verify the accuracy of the model. This facilitates an appropriate comparison between the high-fidelity VTM and the kinematic single-track model.

2.2.1 Verification for Kinematic Model

Two simulations with different speeds were performed with the VTM model. The first simulation setup is a step steer of 2.5° and a longitudinal velocity of tractor is set to be 1 m/s and the second simulation setup is with a step steer of 2.5° and a longitudinal velocity of tractor is set to be 15 m/s. and the articulation angle rates obtained from the VTM were plotted as outputs. In order to compare with the kinematic single-track model, the velocity and steering inputs which were passed to the VTM were provided as input to the kinematic single-track model, and the output articulation angle rates were obtained.

Fig. (2.4a) shows the input velocity and the steering angle for a step steer with the velocity of 1 m/s. The comparison of articulation angle rates between the high-fidelity VTM data and the single-track kinematic model is shown in Fig. (2.4b). The VTM data are displayed by the dotted line, whereas the solid line represents the kinematic model. The similarity between the articulation angle rates determined by the kinematic model and those generated by the VTM indicates a significant amount of agreement between the two models. Since the maneuver is performed at a low speed and the kinematic model uses the VTM input parameters directly, this alignment is expected.

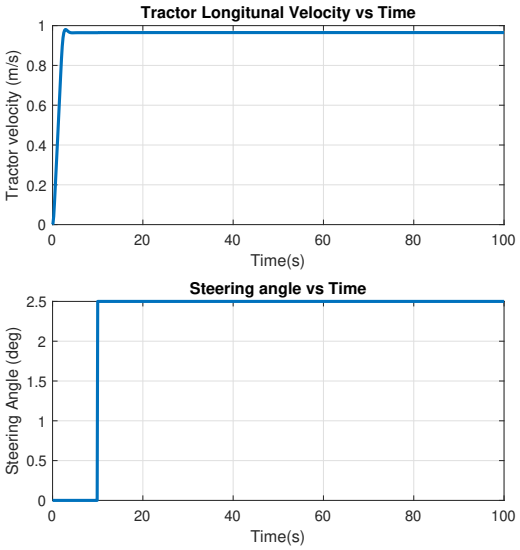

(a) Velocity & steering angle input

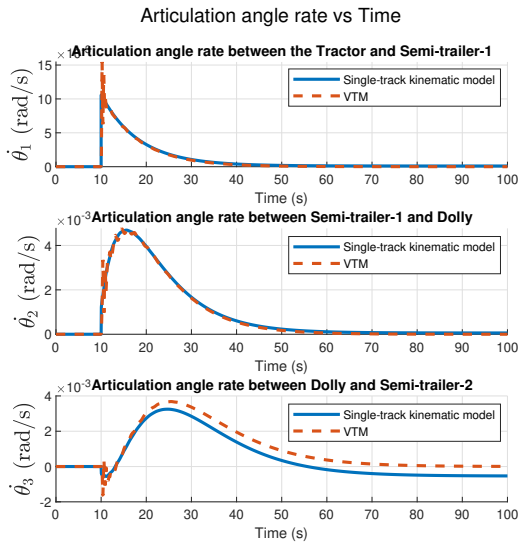

(b) Articulation angle rate vs time

Figure 2.4: Inputs & outputs for a low speed forward maneuver

Fig. (2.5a) shows the input velocity and the steering angle for a step steer with the velocity ramp from 0 to 9.2 m/s from time 0 to 20s. From Fig. (2.5b), it is evident that the kinematic model and the high-fidelity VTM deviate significantly at higher speeds as external forces and inertial effects become more noticeable. This shows the extent to which the kinematic model captures dynamic effects, which become more important as the vehicle speed increases.

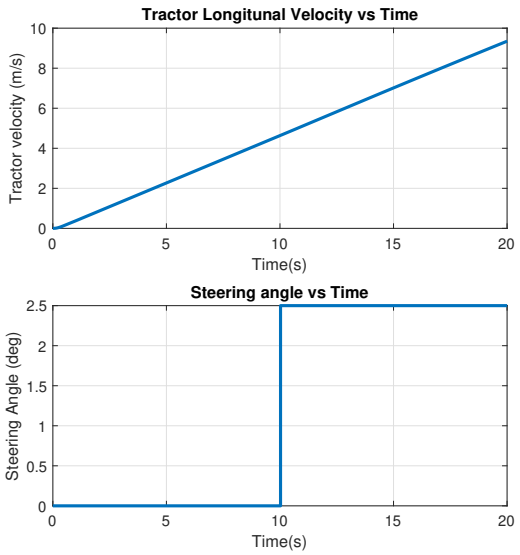

(a) Velocity & steering angle input

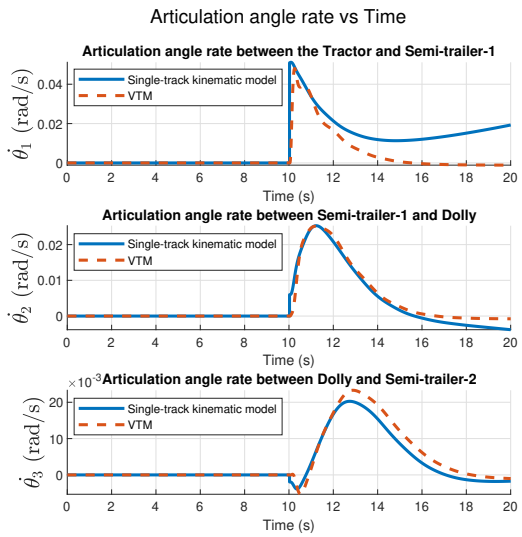

(b) Articulation angle rate vs time

Figure 2.5: Inputs & outputs for a high speed forward maneuver

2.3 Vehicle test with tractor steering

An A-double vehicle shown in Fig. (2.6) was driven with a driver in the loop. During the test, the third axle of the tractor was lifted, as well as the first and third axles of the semi-trailer-2 lifted.

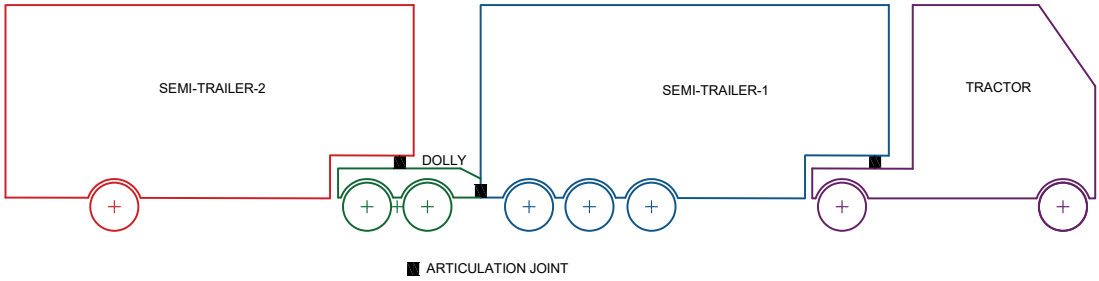

Figure 2.6: Test vehicle configuration

Fig. (2.7) shows the test setup that was used to log the data from the truck. The data from the Vehicle ECU's were read with the help of Controller Area Network (CAN) communication. In order to access the data from the vehicle ECU, CAN breakout harness was made available in the truck. Vector module VN1630A was used as an interface between the laptop and the vehicle to record measurement data such as the steering angle, the vehicle speed, and the yaw-rate of the tractor unit. The truck was then driven with several maneuvers such as forward straight line, forward circular maneuver and reversing at a straight-line.

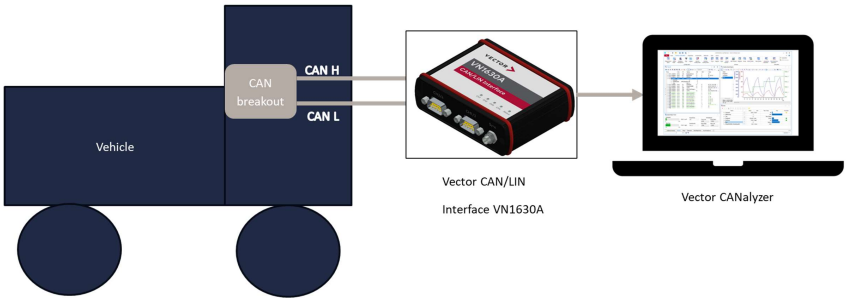

Figure 2.7: Test setup with an A-double truck

2.3.1 Open loop simulation with measured data from A-double combination in Forward direction

The vehicle speed and steering angle were provided as input to the VTM and then the yaw-rate from the VTM was recorded to compare with the vehicle test data and the single-track kinematic model.

The tractor yaw-rate response and the velocity input to the model for a straight-line maneuver are shown in Fig. (2.8) in the forward direction. It could be inferred that the yaw-rate calculated using the single track kinematic model is between 9% and 33% lower than the measured data from the vehicle. It could be because factors such as tire slip, vehicle loads, weight distribution etc. were not taken into account when considering the kinematic single track model. The yaw-rate calculated from the kinematic model converges to $'0'$ as the steering input attempts to, which is consistent with the vehicle data.

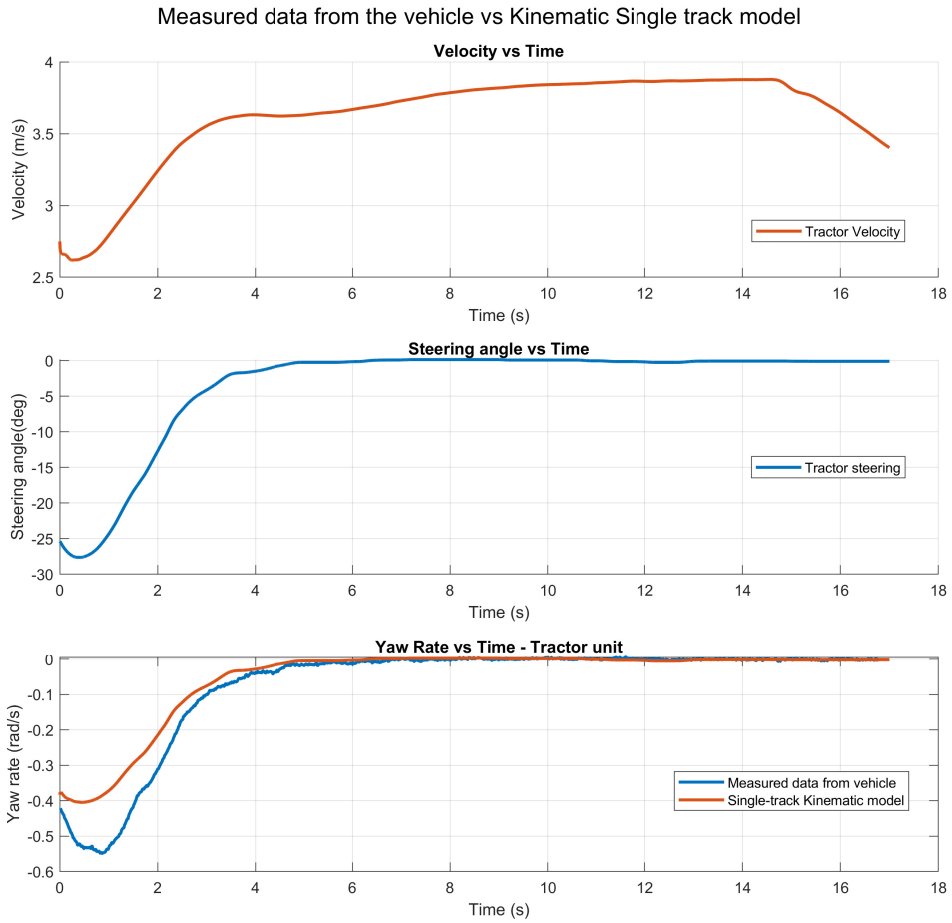

Figure 2.8: Single-track kinematic model validation with real vehicle test data - forward maneuver

2.3.2 Open loop simulation with measured data from A-double combination in Reverse direction

The corresponding response of the yaw-rate is shown in Fig. (2.9) for a reverse maneuver. It can be seen that when the steering angle is closer to zero, the measured yaw-rate and the yaw-rate computed from the single track kinematic model converge, but when the steering angle becomes larger, the computed yaw-rate is $30\,\% \sim 45\,\%$ lower than that of the measured data.

As seen in the figure, the driver reverses the vehicle until approximately 16.5 s. Around 17 s, the driver resumes reversing until 31 s. After 31 s, the driver had to move the vehicle in the forward direction to straighten the configuration. This shows how difficult it is to reverse the A-double vehicle in a straight line.

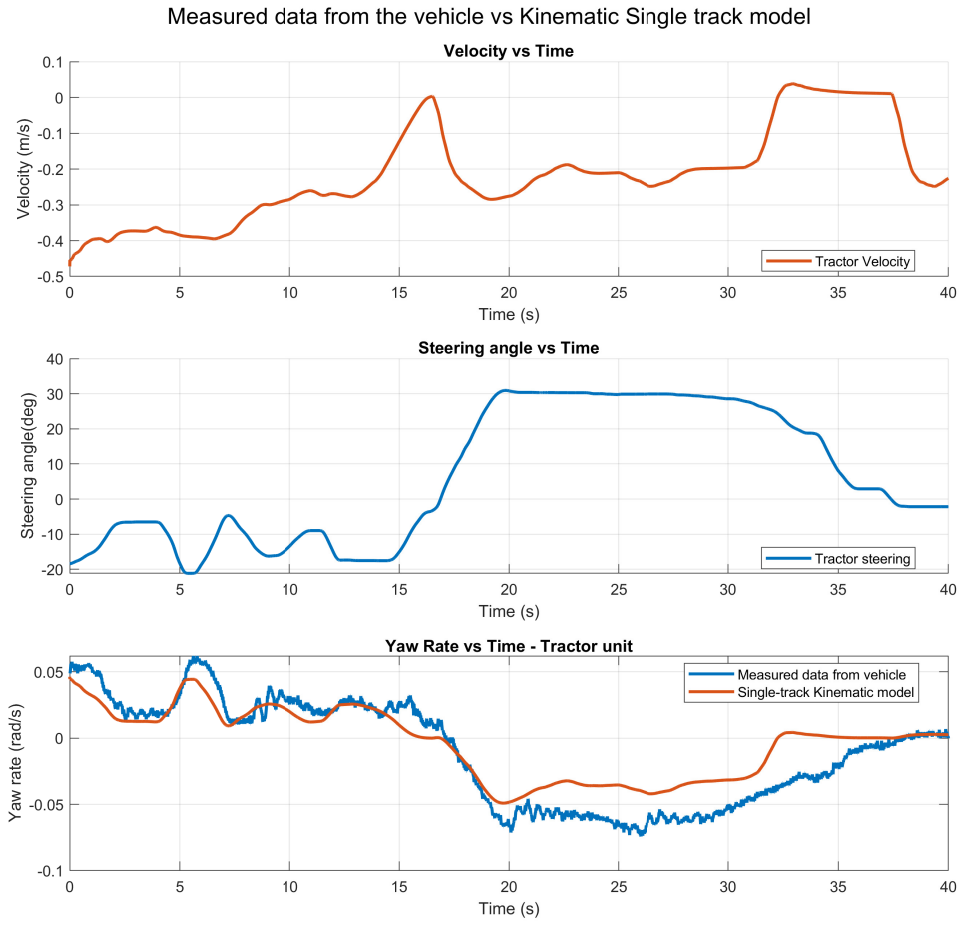

Figure 2.9: Single-track kinematic model validation with real vehicle test data - reverse maneuver

3
Method

This chapter presents the function overview and the controller approach applied for this function to A-double combination vehicle. The mathematical equations derived from the kinematic single-track model in Section (2) form the basis for designing the feedback controller. These equations enable the calculation of control gain parameters essential for maintaining stability and trajectory tracking during reverse maneuvers.

Using this kinematic model presented, a control logic is developed which improves the maneuverability and stability of the A-double combination when reversing. The state space formulation ensures the precise regulation of vehicle articulation angles and trailer alignment, facilitating the accurate desired path set by the driver.

3.1 Function overview

The overview of the function is presented in Fig. (3.1). The driver is equipped with a control knob to specify the desired turning trajectory of the vehicle, either to the left or to the right. This control allows the driver to define the desired turning radius. Upon specification of the radius using the knob, the corresponding desired articulation and steering angles are calculated using a steady state kinematic single-track model. These computed values are subsequently provided as input to the feedback controller.

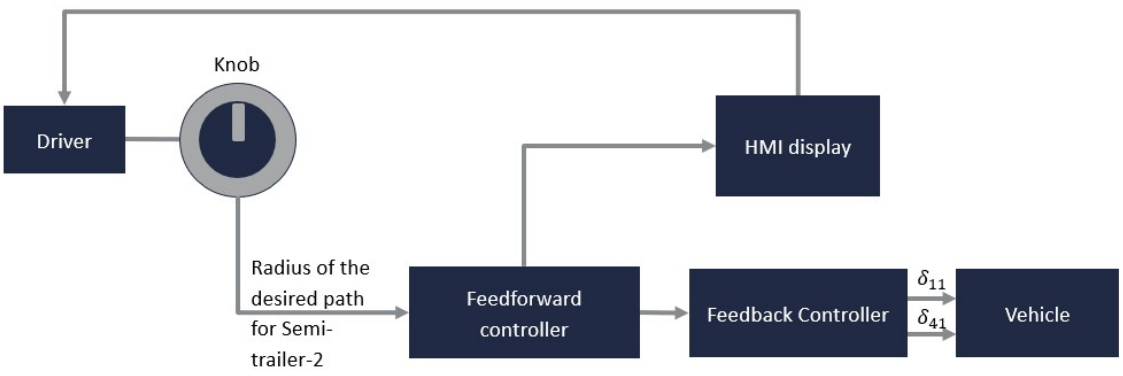

Figure 3.1: Function overview

The feedback controller processes the input and generates the required steering angles δ_{11} and δ_{41}, which are then transmitted to the VTM for execution.

As the driver adjusts the control knob, the predicted trajectory of the vehicle is displayed on the HMI display. Furthermore, if the selected turning radius is not feasible for a A-double combination, a warning will be displayed to the driver on the display and a prompt will be displayed to the driver to reset the control knob to a more feasible value. Any radius value below 10 m is not feasible for this.

3.2 Controller methods

A feedback controller similar to the controller proposed by Rimmer et al. [15] has been used, but instead of steering only the tractor, the method proposed in this work will control two inputs to the steering. One is on the front of the tractor and the other is on the last axle of the Semi-Trailer-2. This dual-steering strategy is expected to provide improved vehicle maneuverability and stability.
This method focuses on the use of two steering angles: δ_{11} for the front axle of the tractor, and δ_{41} for the steering of the last axle of the Semi-Trailer-2. The layout of the control system is illustrated in Fig. (3.2).

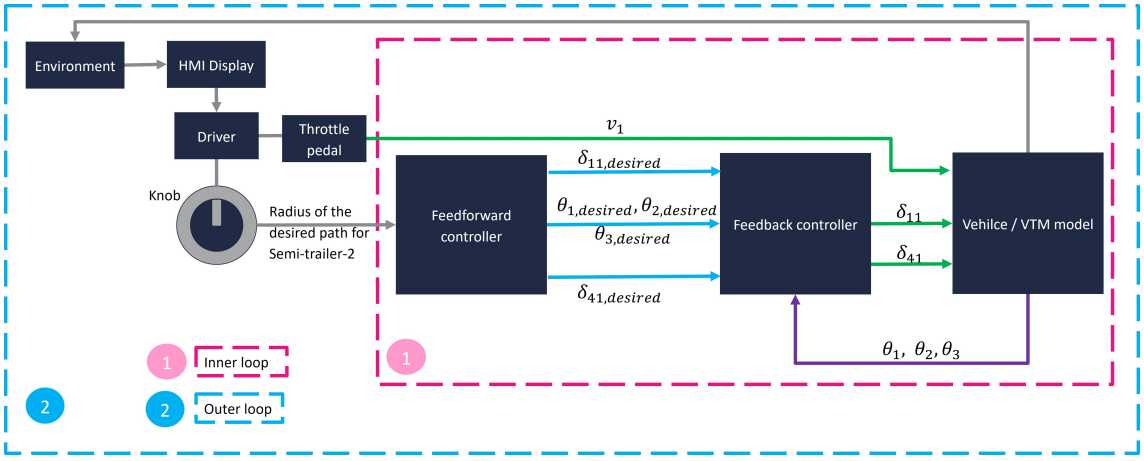

Figure 3.2: Layout of the Controller

The system employs a two-loop structure: an inner loop and an outer loop. The inner loop, as depicted in the figure, primarily addresses the articulation angle deviation and computes the corresponding error. The outer feedback loop is handled by the driver, who is responsible for path planning by setting the desired radius in which the vehicle will have to reverse with the help of the knob.

In the inner loop, the desired radius set by the driver is passed to a function block that contains derived equations based on steady-state kinematic constraints as described in Subsection (3.2.1). Using which the desired articulation angles $\theta_{1,\text{desired}}$, $\theta_{2,\text{desired}}$, $\theta_{3,\text{desired}}$ and the desired steering angles $\delta_{11,\text{desired}}$, $\delta_{41,\text{desired}}$ are obtained en-

suring the end of the Semi-Trailer-2 is following the path.

3.2.1 Feedforward controller

In the Feedforward controller, the articulation angles and the steering angles required to follow the set path are calculated. A steady-state kinematic model is shown in Fig. (3.3). A virtual non-steered axle, represented by a dotted rectangle, is taken into consideration presuming that the driver is interested in positioning the end of the last semi-trailer on the path.

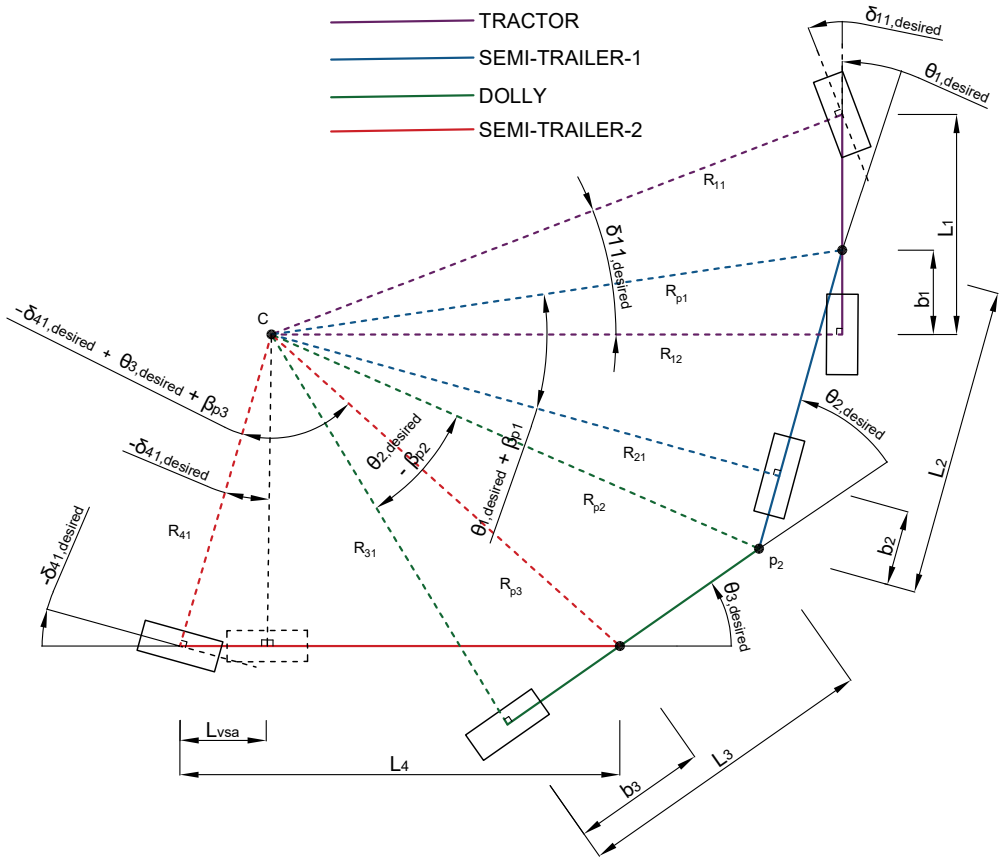

Figure 3.3: Kinematic model for A-double with steerable last trailer

The turning radius of the semi-trailer 2 rear axle is given by,

$$R_{41} = \pm R_{path} \tag{3.1}$$

Note: R_{path} is considered positive for the left turn and negative for the right turn.

The desired steering angle for the Semi-Trailer-2 is calculated by considering a virtual wheel ahead of the last semi-trailer which satisfies the kinematic constraint. Here L_{vsa} is the length of the virtual wheelbase of the last semi-trailer. The steering

angle is given by,

$$\delta_{41,\text{desired}} = -\sin^{-1}\left(\frac{L_{vsa}}{R_{41}}\right) \tag{3.2}$$

The semi-trailer 2 is connected to the dolly through the articulation point p_3 as shown in figure (3.4). Angles A and B are given as follows,

$$A = \tan^{-1}\left(\frac{\frac{L_4}{R_{41}} + \sin(\delta_{41,desired})}{\cos(\delta_{41,desired})}\right) \tag{3.3}$$

$$B = 90° + \delta_{41,desired} - A \tag{3.4}$$

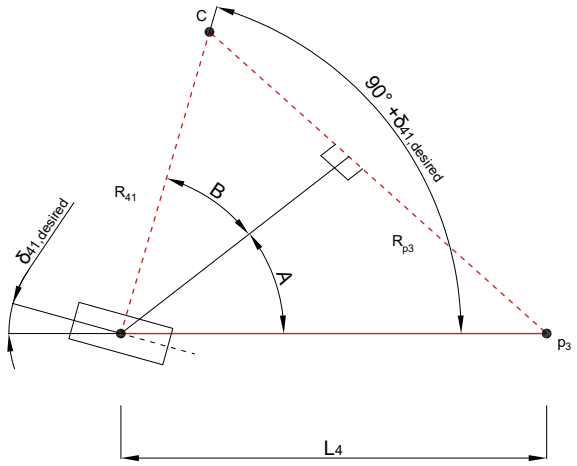

Figure 3.4: Semi-Trailer-2

The turning radius of the point p3 is given by,

$$R_{p3} = L_4 \cdot \sin(A) + R_{41} \cdot \sin(B) \tag{3.5}$$

The turning radius of the dolly rear axle is given by,

$$R_{31} = \sqrt{R_{p3}^2 - b_3^2} \tag{3.6}$$

Slip angle of the dolly is given by,

$$\beta_{p3} = \tan^{-1}\left(\frac{b_3}{R_{31}}\right) \tag{3.7}$$

The desired articulation angle is given by,

$$\theta_{3,\text{desired}} = \tan^{-1}\left(\frac{L_4}{R_{41}}\right) - \beta_{p3} + \delta_{41,\text{desired}} \tag{3.8}$$

The dolly is connected to the semi-trailer 1 via articulation point p_2.

The turning radius of the point p2 is given by,

$$R_{p2} = \sqrt{R_{31}^2 + L_3^2} \tag{3.9}$$

The turning radius of the rear axle of the semi-trailer 1 is given by,

$$R_{21} = \sqrt{R_{p2}^2 - b_2^2} \tag{3.10}$$

The slip angle of the semi-trailer 1 is given by,

$$\beta_{p2} = \tan^{-1}\left(\frac{b_2}{R_{21}}\right) \tag{3.11}$$

The desired articulation angle is given by,

$$\theta_{2,\text{desired}} = \tan^{-1}\left(\frac{L_3}{R_{31}}\right) + \beta_{p2} \tag{3.12}$$

The semi-trailer 1 is connected to the tractor via articulation point p_1.
The turning radius of the point p1 is given by,

$$R_{p1} = \sqrt{R_{21}^2 + L_2^2} \tag{3.13}$$

The turning radius of the rear axle of the tractor is given by,

$$R_{12} = \sqrt{R_{p1}^2 - b_1^2} \tag{3.14}$$

The slip angle of the tractor is given by,

$$\beta_{p1} = \tan^{-1}\left(\frac{b_1}{R_{12}}\right) \tag{3.15}$$

The desired articulation is given by,

$$\theta_{1,\text{desired}} = \tan^{-1}\left(\frac{L_2}{R_{21}}\right) - \beta_{p1} \tag{3.16}$$

The desired steering angle at the front axle of the tractor is given by,

$$\delta_{11,desired} = \tan^{-1}\left(\frac{L_1}{R_{12}}\right) \tag{3.17}$$

3.2.2 Feedback Controller

The kinematic model of an A-double combination vehicle describes the motion of the system in terms of its articulated angles. The articulation angle rates are obtained from the equations (2.32), which form the function equations.

$$f_1 \Rightarrow \dot{\theta}_1 = \dot{\phi}_1 - \dot{\phi}_2 \tag{3.18}$$

$$f_2 \Rightarrow \dot{\theta}_2 = \dot{\phi}_2 - \dot{\phi}_3 \tag{3.19}$$

$$f_3 \Rightarrow \dot{\theta}_3 = \dot{\phi}_3 - \dot{\phi}_4 \tag{3.20}$$

3.2.2.1 Linearization

In order to obtain a linear model, the vehicle has been linearized along a straight line. Hence, we apply the small-angle approximation as shown in Eq. (3.21) to the non-linear kinematic equations Eq. (3.18),(3.19) and (3.20).

$$\sin\theta \approx \theta, \quad \cos\theta \approx 1, \quad \tan\theta \approx \theta, \quad \arctan\theta \approx \theta \tag{3.21}$$

The general form of the nonlinear system is given by:

$$\dot{x} = f(x, u) \tag{3.22}$$

where:

- $x = [\theta_1, \theta_2, \theta_3]^T$ is the state vector.
- $u = [\delta_{11}, \delta_{41}]^T$ is the input vector.

The simplified system is then used to perform Jacobian linearization. The **Jacobian linearization** involves computing the partial derivatives of $f(x, u)$ with respect to X and u at the equilibrium point:

$$A = \left.\frac{\partial f}{\partial x}\right|_{(x_0,u_0)} \tag{3.23}$$

$$B = \left.\frac{\partial f}{\partial u}\right|_{(x_0,u_0)} \tag{3.24}$$

Since the vehicle will be linearized along a straight line, the equilibrium point is at $x_0 = [0, 0, 0]^T$ and $u_0 = [0, 0]^T$, where $\dot{x} = 0$.

Performing the differentiation yields the following system matrices.

$$A = \left.\begin{bmatrix} \frac{\partial f_1}{\partial \theta_1} & \frac{\partial f_1}{\partial \theta_2} & \frac{\partial f_1}{\partial \theta_3} \\ \frac{\partial f_2}{\partial \theta_1} & \frac{\partial f_2}{\partial \theta_2} & \frac{\partial f_2}{\partial \theta_3} \\ \frac{\partial f_3}{\partial \theta_1} & \frac{\partial f_3}{\partial \theta_2} & \frac{\partial f_3}{\partial \theta_3} \end{bmatrix}\right|_{x_0,u_0} \tag{3.25}$$

$$B = \left.\begin{bmatrix} \frac{\partial f_1}{\partial \delta_1} & \frac{\partial f_1}{\partial \delta_2} \\ \frac{\partial f_2}{\partial \delta_1} & \frac{\partial f_2}{\partial \delta_2} \\ \frac{\partial f_3}{\partial \delta_1} & \frac{\partial f_3}{\partial \delta_2} \end{bmatrix}\right|_{x_0,u_0} \tag{3.26}$$

These matrices define the **linearized state-space model**:

$$\dot{x} = Ax + Bu \tag{3.27}$$

Up on performing the Jacobian linearization the following A and B matrix are obtained.

$$A = \begin{bmatrix} -\frac{v_1}{L_2} & 0 & 0 \\ \frac{v_1(L_1 b_2 + L_1 L_3)}{L_1 L_2 L_3} & -\frac{v_1}{L_3} & 0 \\ -\frac{v_1(L_1 L_4 b_2 - L_1 b_2 b_3)}{L_1 L_2 L_3 L_4} & \frac{v_1(L_1 L_2 L_4 - L_1 L_2 b_3)}{L_1 L_2 L_3 L_4} & -\frac{v_1}{L_4} \end{bmatrix}$$

$$B = \begin{bmatrix} \frac{v_1(L_2 - b_1)}{L_1 L_2} & 0 \\ \frac{v_1(L_3 b_1 + b_1 b_2)}{L_1 L_2 L_3} & 0 \\ -\frac{v_1(L_4 b_1 b_2 - b_1 b_2 b_3)}{L_1 L_2 L_3 L_4} & \frac{v_1}{L_4} \end{bmatrix}$$

3.2.2.2 Controller gain computation using LQR

The Linear Quadratic Regulator (LQR) is used to design an optimal state feedback controller that minimizes the following cost function:

$$J = \int_0^\infty \left(x^T Q x + x^T R x \right) dt$$

where:

- Q is a positive semi-definite matrix that penalizes deviations in the state vector,
- R is a positive definite matrix that penalizes the control input.

For the system described in Eq. (3.27), we define the following matrices for the LQR design:

$$Q_{\text{lqr}} = \begin{bmatrix} Q_{11} & 0 & 0 \\ 0 & Q_{22} & 0 \\ 0 & 0 & Q_{33} \end{bmatrix}$$

Where $Q_{11},\ Q_{22}$ & Q_{33} are the weights for the state vector.

$$R_{\text{lqr}} = \begin{bmatrix} R_{11} & 0 \\ 0 & R_{22} \end{bmatrix}$$

Where R_{11} & R_{22} are the weights for the input vector.

The weights of the state vector and the input vectors are tuned for different vehicle test setups

Optimal state feedback gain matrix K is computed based on the system's dynamics and the desired weighting in Q_{lqr} and R_{lqr}. The `lqr` function in MATLAB was used, which solves the continuous-time algebraic Riccati equation (CARE) and computes the optimal gain:

$$[K, \sim, \sim] = \text{lqr}(sys, Q_{\text{lqr}}, R_{\text{lqr}})$$

where sys represents the linearized state-space system $\dot{X} = Ax + Bu$, and K is the resulting gain matrix.

3.3 Human-Machine Interface for Reversing Assistance

The Human-Machine Interface (HMI) is developed as a critical component for enhancing driver awareness and support during complex reversing maneuvers of an A-double combination vehicle. The HMI provides a real-time visual representation of the articulated vehicle's state, trajectory prediction, and error feedback. This system is particularly tailored to support low-speed reverse driving scenarios, where articulation angles and trailer tracking dynamics are non-trivial and require precise control and visual feedback.

3.3.1 System Architecture Overview

The architecture of the HMI system integrates three primary components:

- **Simulink-based Vehicle Dynamics and Control Model** (Vehicle Transport Model with Controller)
- **C++ Interface Layer for Real-Time Execution**
- **Visualization and Interaction Layer using Unreal Engine 5**

The interconnection between these subsystems ensures tight coupling between the physics-based simulation and the visualization environment.

3.3.2 Vehicle Dynamics Model and Controller Integration

The foundation of the reversing logic lies in the model *VTM* developed in Simulink. This model consists of two main components: the plant model (the VTM) and the controller. This model simulates the kinematics and dynamics of a multi-body articulated vehicle (A-double combination), including joint articulation, trailer yaw angles,roll, pitch and speed dynamics.

The control system implements a trajectory-following algorithm that computes steering commands based on a desired trajectory path, provided via driver input using a knob. To interface the Simulink model with Unreal Engine, the complete model and controller are compiled into a shared dynamic library (*.dll* file) using *Simulink Coder*. This process also produces a `.lib` file, which includes the controller and exposes various inputs (e.g., velocity request and curvature) and outputs (e.g., pose, articulation angles, and predicted trajectory).

This compiled module is linked within the Unreal Engine framework for real-time co-simulation.

3.3.3 Unreal Engine-Based Visualization

The graphical representation of the A-double vehicle combination is constructed using *Unreal Engine 5*, leveraging its real-time rendering and physics animation capabilities.

Vehicle Model Representation

A detailed *3D model* of the A-double combination is imported as a skeletal mesh in Unreal Engine. The model is animated based on real-time state data from the VTM simulation. `VTMMovementComponent` is the one stepping the simulation and copying outputs to the mesh transform.

Blueprint Integration

UE5's Blueprint system Fig. (3.5) facilitates user interaction and state synchronization. The driver's input (control knob) is captured via a user interface and passed to the simulation layer. Updated vehicle states are rendered each frame, enabling real-time visual consistency with the underlying physical model.

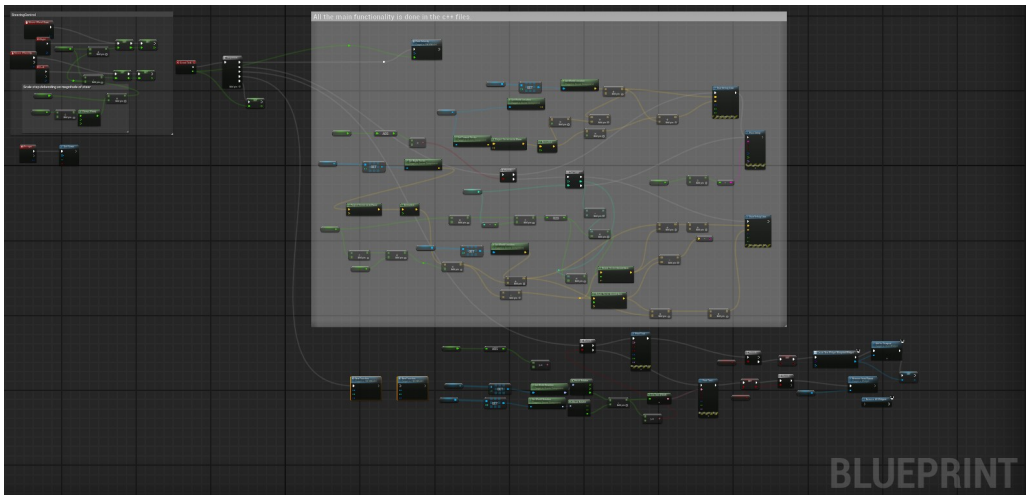

Figure 3.5: Representation of Blueprint layout

3.3.4 Trajectory Prediction and Visualization

A key feature of the Human-Machine Interface (HMI) display is the visualization of the vehicle's trajectory, which is set by the user during reversing maneuvers. The driver defines this trajectory starting from the midpoint of the rear axle of Semi-trailer-2. The HMI display provides the user with relevant information, including speed, turning radius (as set using the control knob), the articulation angle between the dolly and Semi-trailer-2, and the actual path taken by Semi-trailer-2.

Utilizing the current articulation states and steering input, the controller computes a curvilinear path. This path is rendered in Unreal Engine using spline components to depict the trajectory arc. The trajectory is updated continuously to reflect real-time changes in driver input and vehicle dynamics.

The HMI visualization for a straight-line trajectory is presented in Fig. (3.6), while the visualization corresponding to a curved path is shown in Fig. (3.7).

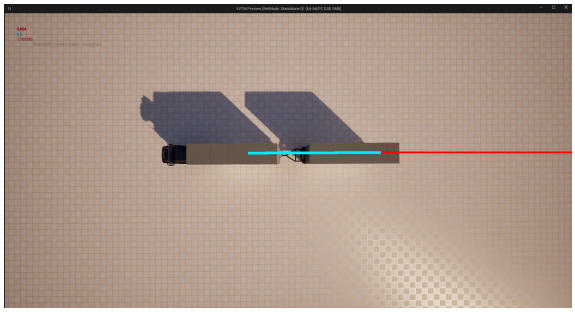

Figure 3.6: Visual representation of vehicle combination to the user from the HMI display while straight line reverse

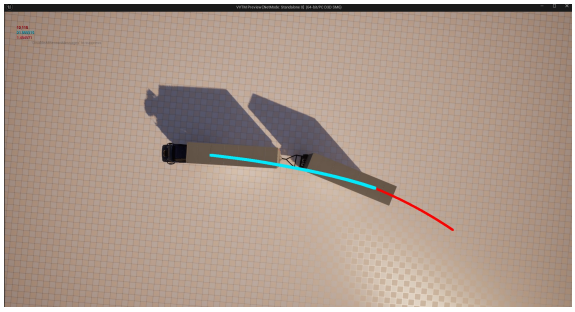

Figure 3.7: Visual representation of vehicle combination to the user from the HMI display while making a circular reverse

In Fig. (3.6) and (3.7), the top-left section of the screen displays key driving information for the user. The red line, which originates at the midpoint of the rear axle of Semi-trailer-2, represents the intended trajectory as set by the user using the control knob. The cyan-colored line indicates the path traced by the semi-trailer-2 unit based on the control knob input provided by the driver.

3.3.5 Real-Time User Information and Safety Warnings

To ensure safe maneuvering of the vehicle combination, the Human-Machine Interface (HMI) display provides the following real-time information:

- **Articulation Angle Information:** Displays the real-time articulation angle between the dolly and the second semi-trailer (Semi-Trailer 2).

- **Radius Input:** Shows the real-time turning radius as set by the user via the control knob.

- **Velocity:** Indicates the real-time longitudinal velocity of the vehicle in meters per second (m/s).

- **Warning Notification:** If the real-time articulation angle between the dolly and Semi-Trailer 2 satisfies the warning condition (see Condition 3.3.5), a warning message is displayed. The message instructs the driver to stop the vehicle and proceed forward to realign the vehicle combination. Simultaneously, the articulation angle display is replaced with the warning text: *"Warning! Stop and move forward."*

  Condition for Warning notification: When the articulation angle between the dolly and the Semi-trailer-2 reaches greater than or equal to 25 deg [17].

In the Fig. (3.8), here is the example of how the real-time information is displayed. the serial number 1 indicates the articulation angle, next is the Radius input, and the last is the vehicle velocity.

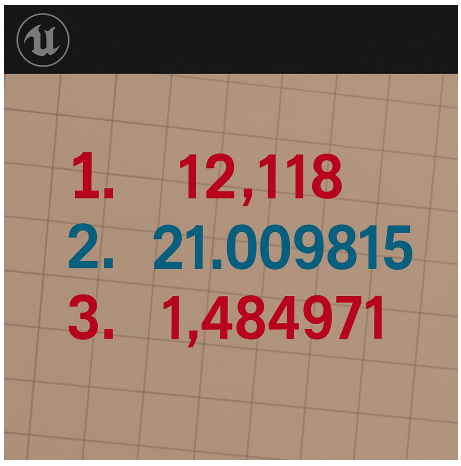

Figure 3.8: Information provided on display for user

In Fig. (3.9), an example of how the warning notification is displayed is shown. As observed, the real-time articulation angle information is replaced by a warning notification when the specified condition (3.3.5) is met.

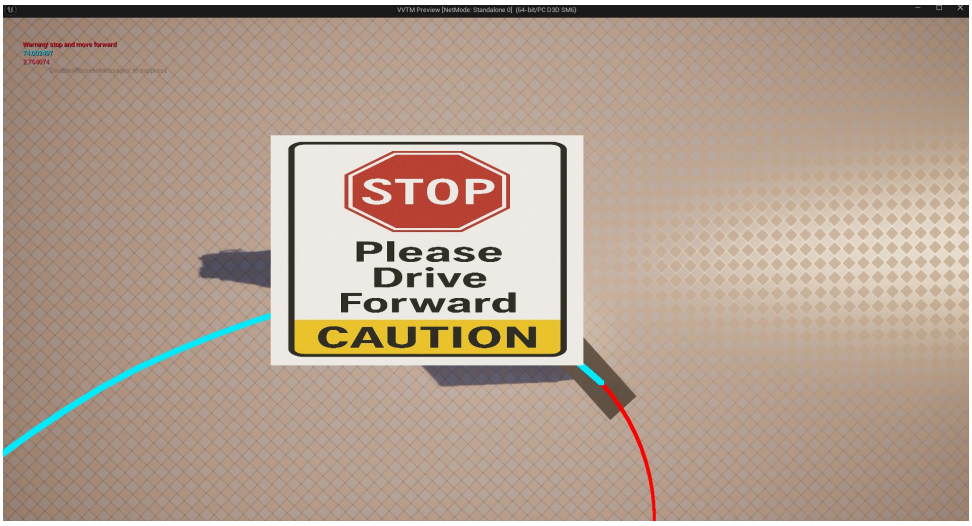

Figure 3.9: Warning notification displayed

Once this warning appears, the driver must take the necessary action, which is to stop the vehicle and then drive forward to straighten the vehicle combination.

This HMI system effectively integrates a Simulink-based vehicle and controller model with high-fidelity visualization in Unreal Engine. Its modular design and robust real-time user information and safety warnings provide intuitive support for drivers during reverse maneuvers involving complex combinations of articulated vehicles. The architecture also supports extensibility for broader ADAS applications and training simulators.

3.4 Performance Metrics

This section defines the performance-based characteristics of the long combination vehicles, which are used later to validate the results.

- **Off-tracking (or) tractor swing:** Off-tracking or tractor swing refers to the phenomenon in which the path of the trailer's rear wheels diverges from the path of the tractor's front wheels at steady state. This deviation occurs as the vehicle units are articulated during turning. Off-tracking is further exacerbated when reversing, as the articulation of the tractor-trailer unit becomes more pronounced, making it increasingly difficult to maintain alignment between both units. The unit is meters.

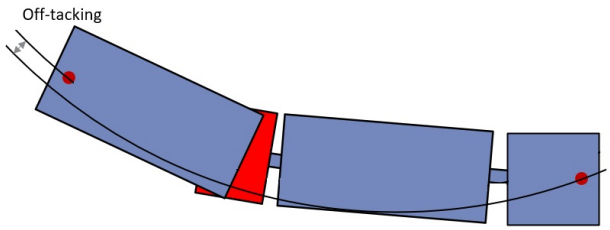

Figure 3.10: Off-tracking for A-double combination

- **Total Steering Correction (TSC):** refers to the *cumulative sum of all steering adjustments* made to maintain a desired path. The unit is Radians

  Given the steering angle at each time step θ_i and the total number of time steps N:

$$\text{TSC} = \sum_{i=1}^{N} |\Delta\theta_i| = \sum_{i=1}^{N} |\theta_i - \theta_{i-1}|$$

  - $\Delta\theta_i$: Steering correction at time step i
  - Absolute value ensures all corrections (left or right) contribute positively
  - **Higher TSC** $\Rightarrow$ More frequent or larger corrections (Indicates instability or poor path tracking)
  - **Lower TSC** $\Rightarrow$ Smoother steering (Suggests good control and stability)

  There are three TSC that have been used to compare the steering configuration that has been proposed in this thesis.
  - TSC_1 $\Rightarrow$ Total steering correction made by tractor steering.
  - TSC_2 $\Rightarrow$ Total steering correction made by the steering of the semi-trailer-2.
  - TSC_{total} $\Rightarrow$ Total steering correction made when using both steering inputs are used.

$$TSC_{total} = TSC_1 + TSC_2$$

- **Quickness:** It denotes the response of a vehicle in completing a specified maneuver in the shortest possible time, without compromising stability or inducing jackknifing. It is expressed in seconds.

- **Transient Swept Width (TSW):** The transient swept width represents the peak-to-peak deviation of the tractor's trajectory alone during a transient maneuver, which occurs when changing from one steady state to another (such as a sharp turn or lane change) as shown in Fig. (3.11). It is expressed in meters.

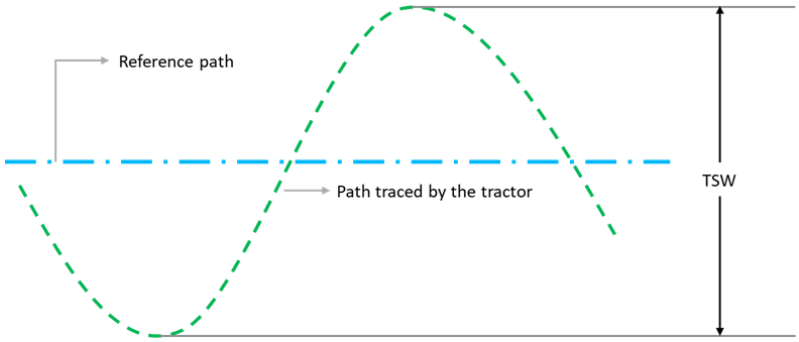

Figure 3.11: Transient Swept Width of the tractor

3.5 Test cases

The test case defined in this subsection will be used to validate the truck with tractor steered vehicle with & without semi-trailer-2 steered in different maneuvers and different load cases which is summarized in the Table (3.1).

Trajectory Reference:
The radius input used in the test case to execute the desired maneuver is time-based and manually tuned for each specific scenario. The custom-developed function `get_radius_ref(t)` generates a reference radius profile over time, assigning distinct values—such as infinity for straight segments and a constant finite radius for turning segments—according to defined time intervals.

Maneuver:
The following three maneuvers were considered to test and compare the different models and steering configurations that we have.

1. **Circle Maneuver:** The vehicle starts from a standstill position with zero articulation angles and follows a circular path with a radius of 30 m.

2. **Straight line Maneuver:** The A-double combination begins from a steady-state curve with constant articulation angles and then follows a straight line which has a length of 200 m.

3. **Combined Maneuver:** The test case depicted in Fig. (3.12) consists of a combination of four 100 m long straight segments, a circular section with a 50 m radius, and two 90° turns with a radius of 12.5 m.

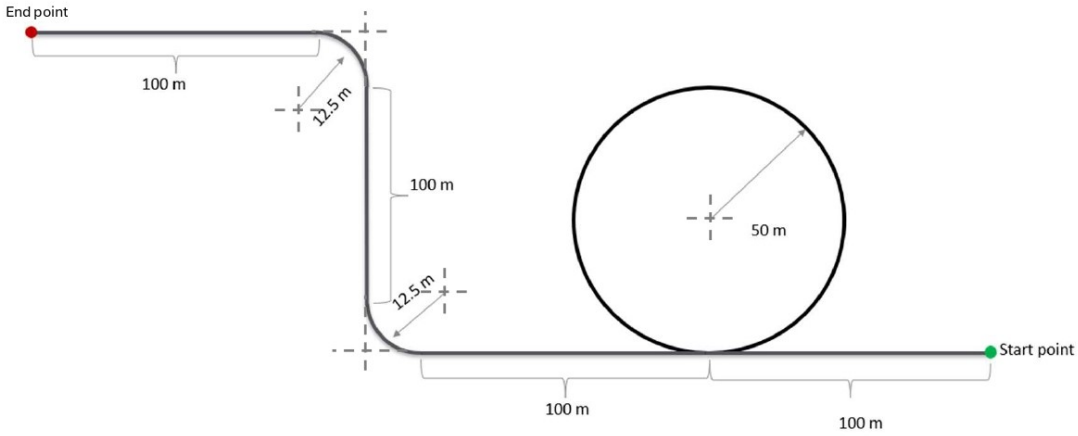

Figure 3.12: Combined Maneuver

Steering configuration:
There are two configurations of steering that will be tested.

1. Tractor front axle steered

2. Tractor front axle steered and the last axle of the Semi-Trailer-2 steered

Type of axle configuration:
There are two types of vehicles that are set up in VTM that will be used for testing.

1. Vehicles with grouped non-steerable axles. as depicted in Fig. (2.2) which is referred as Lumped model.

2. Vehicles without grouped non-steerable axles. as depicted in Fig.(2.1) which is referred as All axle model.

Load case:
In order to study the effect of laden and unladen mass, in some of the simulation test cases, the Semi-trailer-1 was unloaded.

1. **Laden mass:** For the lumped model case, the axle load on semi-trailer 1 is 6.4 tons. In the all axle model, each of the three axles on semi-trailer 1 are equally loaded with 6.6 tons.

2. **Unladen mass:** This case was tested only with the model in which all axles were considered. Each of the three axles on semi-trailer 1 is equally loaded with 1.7 tons, totaling 5.1 tons.

Summary of the Test cases:

Test case	Maneuver			Steering		Type of axle configuration		Load case	
	Circle	Straight	Combined	Tractor	Semi-Trailer-2	Lumped	All-Axle	Laden	Unladen
1	✓			✓		✓		✓	
2	✓			✓	✓	✓		✓	
3	✓			✓			✓	✓	
4	✓			✓	✓		✓	✓	
5	✓			✓			✓		✓
6	✓			✓	✓		✓		✓
7		✓		✓		✓		✓	
8		✓		✓	✓	✓		✓	
9		✓		✓			✓	✓	
10		✓		✓	✓		✓	✓	
11		✓		✓			✓		✓
12		✓		✓	✓		✓		✓
13			✓	✓			✓	✓	
14			✓	✓	✓		✓	✓	

Table 3.1: Test cases for comparing Performance metrices

3.6 Normalization Technique

The Min-Max normalization technique will be applied to compare the data from the maneuver with different steering configuration.

Min-Max Normalization:
It is an easy approach to compare the data set with the expectation that the original relationship of the data would be retained. In the Min-Max Normalization process, the rescaling usually occurs in the range of [0,1] or [-1,1]. [0,1] will be followed, where 0 represents the lowest value in the data set and 1 represents the highest value in the data set. The expression for normalization is as follows:

$$z' = \frac{z - z_{\min}}{z_{\max} - z_{\min}} \tag{3.28}$$

where z' is the normalized value, z is the original value, and $z_{\min}$ and $z_{\max}$ are the minimum and maximum characteristic values of the data set.

4
Results

The controller developed in Section (3) is implemented using the VTM as the plant model. The VTM model was modified to represent both the lumped-axle model and a configuration where all axles are considered individually. This setup constitutes a closed-loop system simulation in which the system's response is continuously adjusted to achieve the desired output. The simulation captures the behavior of the system for different test case scenarios.

4.1 Results for the Test Cases

The plant model was simulated with a velocity of 1 m/s in the reverse direction. Four distinct gains in the controller were used based on the type of steering and the type of model.

In the results shown below, the images on the left column depict the test cases in which only the tractor is steered. The images on the right column show the test cases where both the tractor and semi-trailer-2 are steered.

The trajectories presented in the results are measured from the midpoint of the front axle of the tractor. For semi-trailer-2, the measurement is taken from the midpoint of the steerable axle.

4.1.1 Circle maneuver

Test case 1 & 2:
In test case 1 & 2, the truck was simulated with the lumped model in a circle maneuver of radius 30 m. It is evident from the steering input in Fig. (4.1a) that when the tractor is steered alone, the input generated by the controller remains in the transient phase for approx. 75 seconds before the system reaches a steady state. The peak-to-peak swing of the steering input is about 24°. As a result, the articulation angles, primarily at the articulation angles 1 and 2, exhibit a behavior that is similar to that of the steering input, which can be seen in Fig. (4.1b). However, the input to the model is smoother when both the tractor and the semi-trailer-2 steering inputs are used, with the peak-to-peak value of the tractor steering input is around4.2° (which is 82.5% lower than that of the test case 1) and for the semi-trailer-2, it is around 13.4°. It approaches steady state around 45 seconds when both steering are

used, resulting in a smoother transition at the articulation angle.

The path followed by the tractor and the semi-trailer-2 and TSW for both test cases are shown in Fig. (4.1c) & (4.1d). In this, it is evident that the tractor has peak-to-peak swept width of 3 when only the tractor steering is used, but when both the steering inputs are used peak-to-peak swept width was reduced to 1.39 m which is nearly 58.6% reduction.

Test case 3 & 4:
In the test case 3 & 4, all axle was simulated in a circle maneuver of radius 30 m. From the input responses shown in Fig. (4.2a) it can be seen that, in both the test case 3 & 4, the tractor steering is oscillatory until it reaches the steady state. But the peak-to-peak steering angle is 34° when the steering input is only provided by the tractor, whereas when both the steering inputs are provided, the peak-to-peak steering angle is 27°, which is 20.6% lesser when compared with the tractor only steered case. The response to the articulation angles exhibits a similar response to that of the steering input as seen in Fig. (4.2b) and the controller output eventually approaches the steady state.

In both test cases, the tractor steering reaches steady state in about 150 seconds. It could be because all the axles are included, due to which the system dynamics increases. The semi-trailer-2 has a maximum peak-to-peak steering angle of 22° and reaches steady state at around 140 seconds.

The path followed by the tractor and the semi-trailer-2 and TSW for both test cases are shown in Fig. (4.2c) & (4.2d) respectively. The tractor swing is higher in all axle model when compared to the lumped model. The path of the tractor has a swept width of 4.41 m when only the tractor steering is used, but when both steering inputs are used, the swept width was reduced to 3.96 m as shown in Fig. (4.2d), which is only 10% reduction. Using all axle model, the swept width increases by 48% compared to the lumped model, which is expected.

Test case 5 & 6:
In test case 5 & 6, all axle with unladen mass on the semi-trailer-1 were simulated in a circle maneuver of radius 30 m. Fig. (4.3a) shows the steering generated by the controller. Similar to the test case 3 & 4, the steering inputs are oscillatory but the steady state is reached even faster with the same controller gain at around 110 seconds with the peak-to-peak steering angle of 27° when only tractor is steered and approximately around 75 seconds with the peak-to-peak steering angle of 15° when both steering inputs are provided. The steering of the semi-trailer-2 is reaches steady state around 75 seconds with the peak-to-peak steering of 14°. The articulation angles, which can be seen in Fig. (4.3b), seem to follow the input steering response similar to the laden case.

Fig. (4.3c) shows the path of the tractor and the semi-trailer-2 and Fig. (4.3d), shows the TSW plot. When steering on the tractor alone used, the TSW is 11.5%

lower than that of the laden case. For the tractor with semi-trailer-2 case, the TSW is 39.8% lower than the laden case.

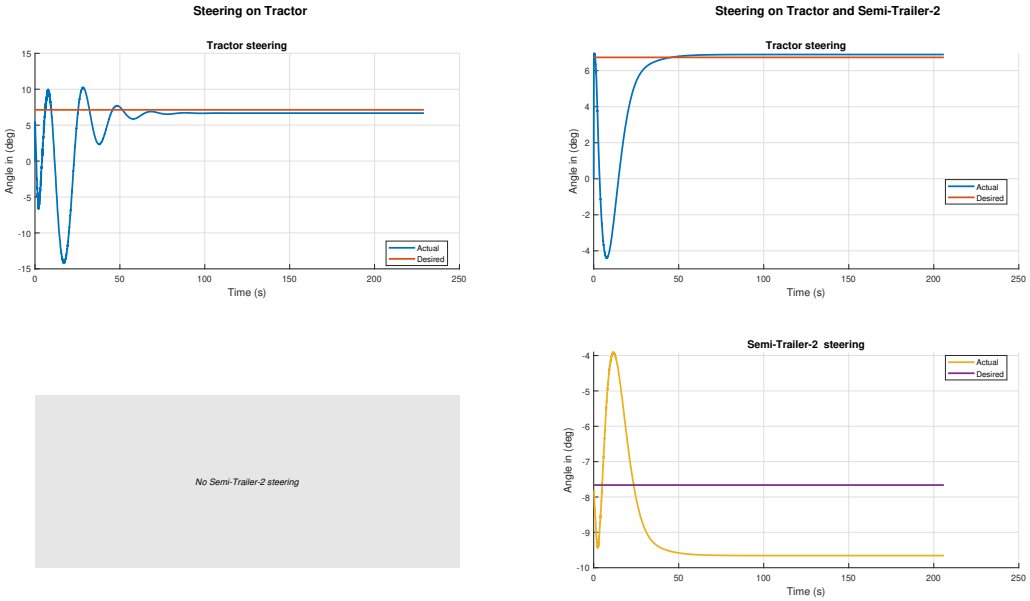

(a) Steering angle input

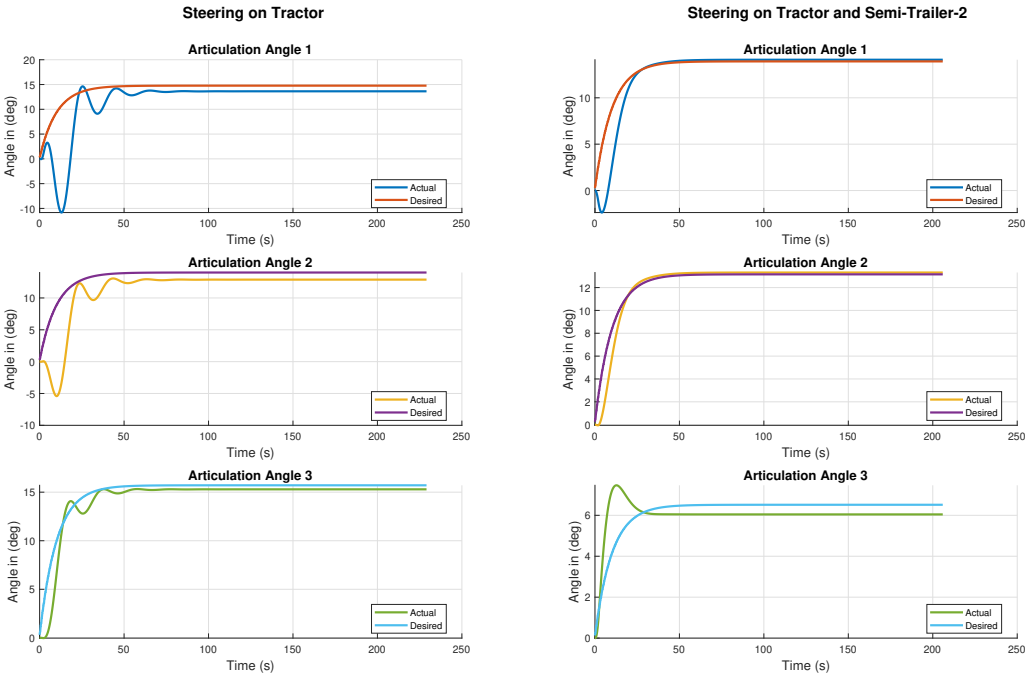

(b) Articulation angle output

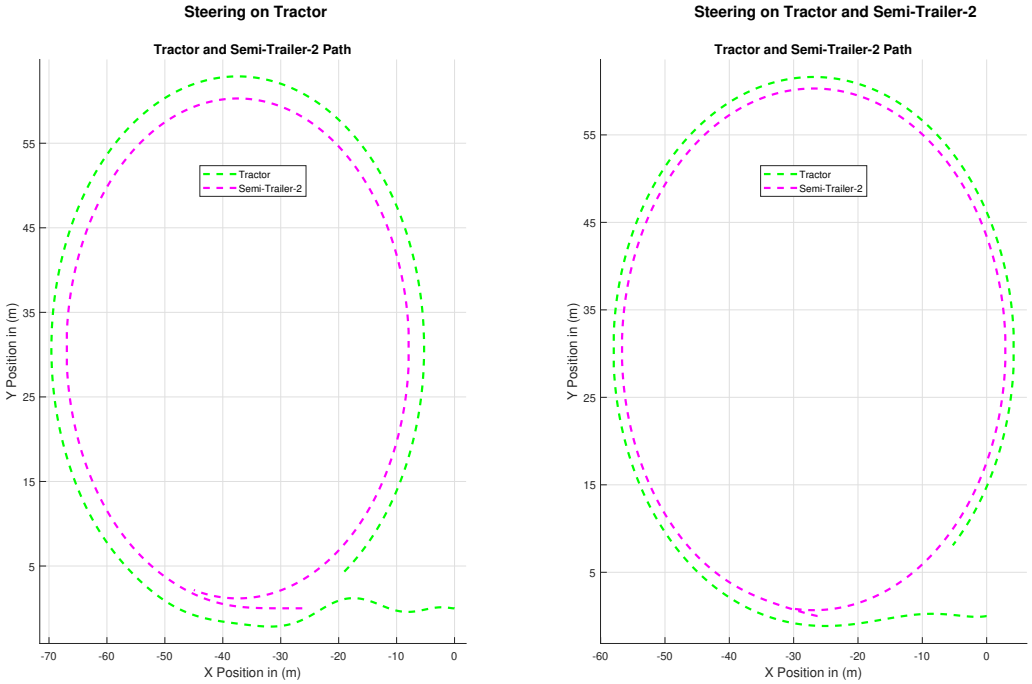

(c) Path of the Tractor and the Semi-trailer-2 while reversing

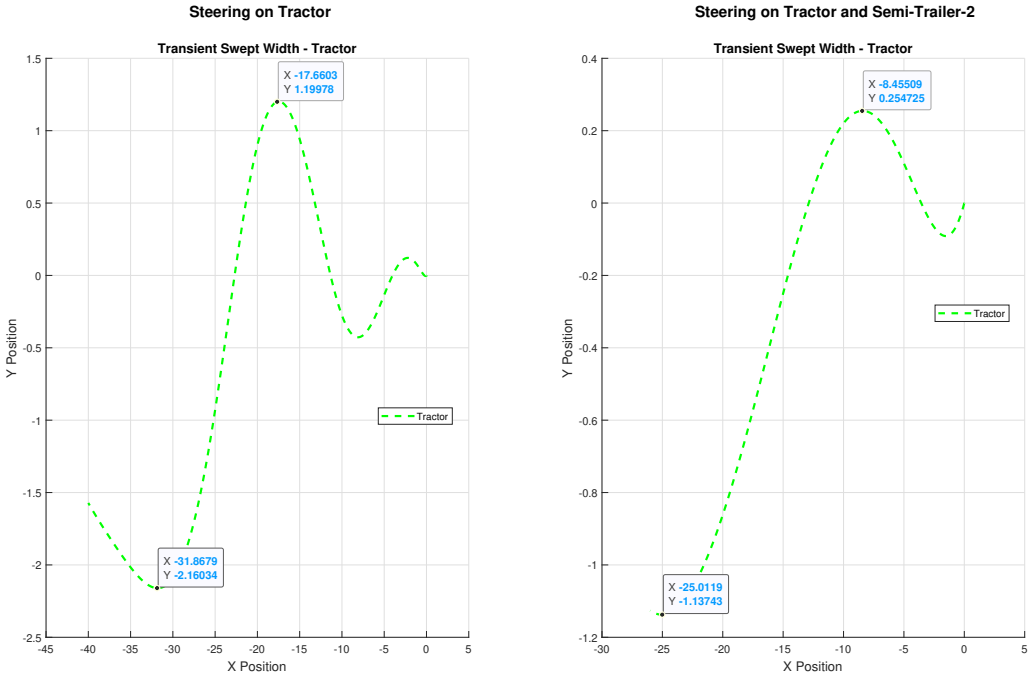

(d) Transient Swept Width of Tractor

Figure 4.1: Steering input, Articulation angle output, Path and Transient Swept width for test case 1 & 2

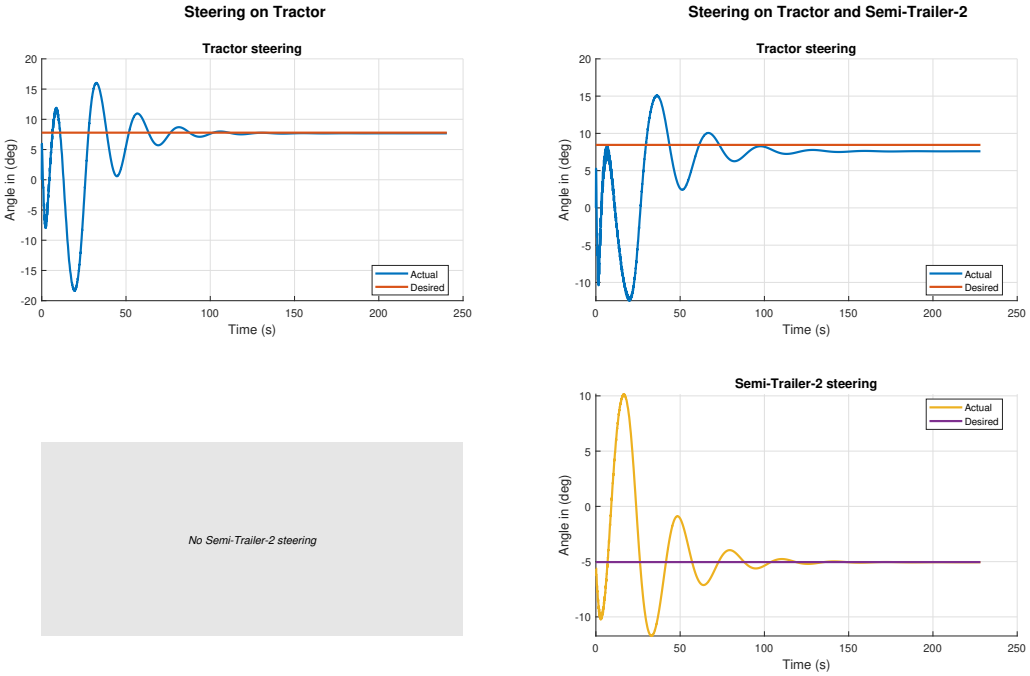

(a) Steering angle input

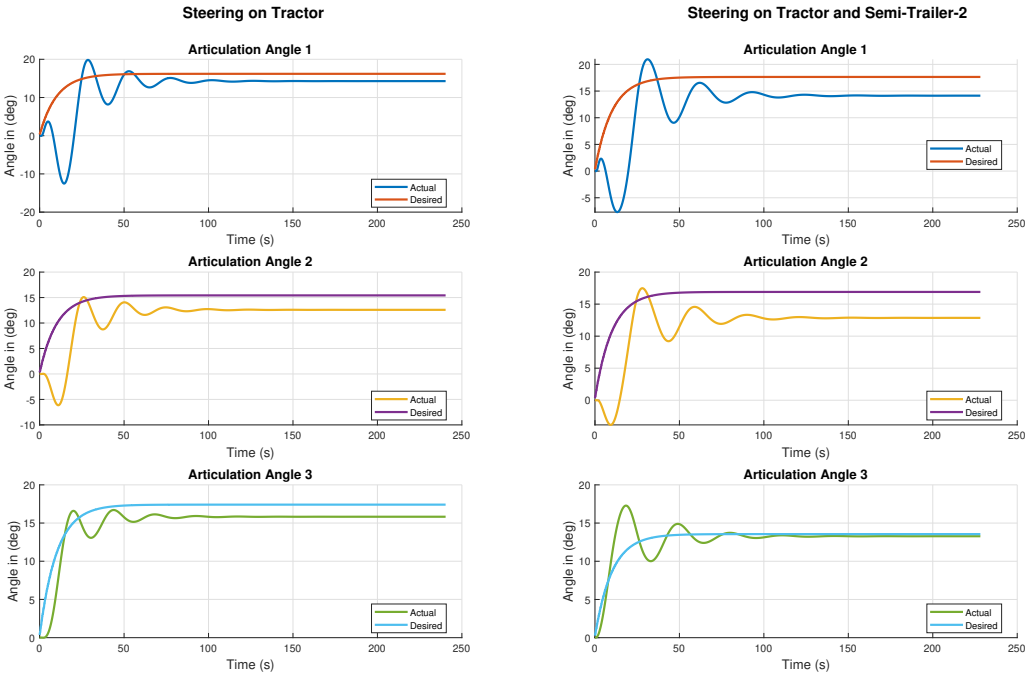

(b) Articulation angle output

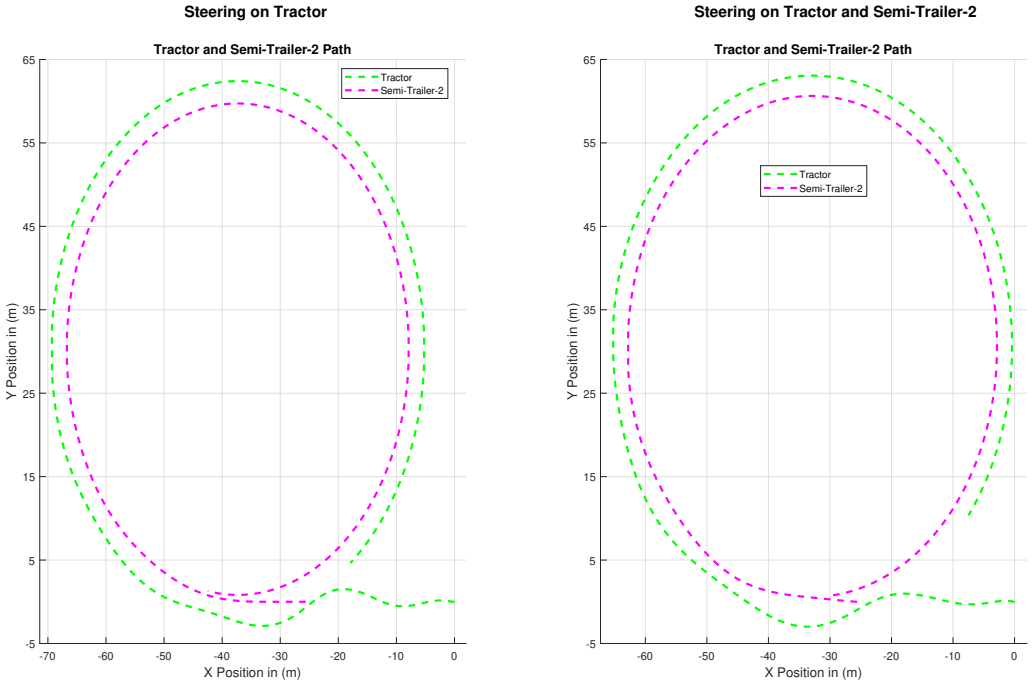

(c) Path of the Tractor and the Semi-trailer-2 while reversing

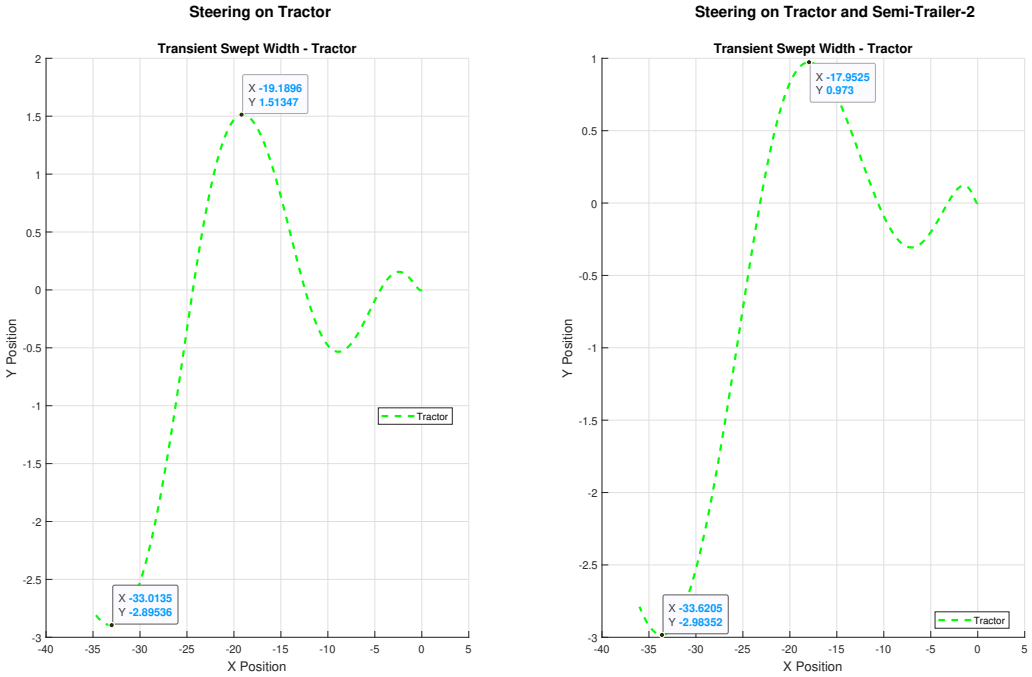

(d) Transient Swept Width of Tractor

Figure 4.2: Steering input, Articulation angle output, Path and Transient Swept width for test case 3 & 4

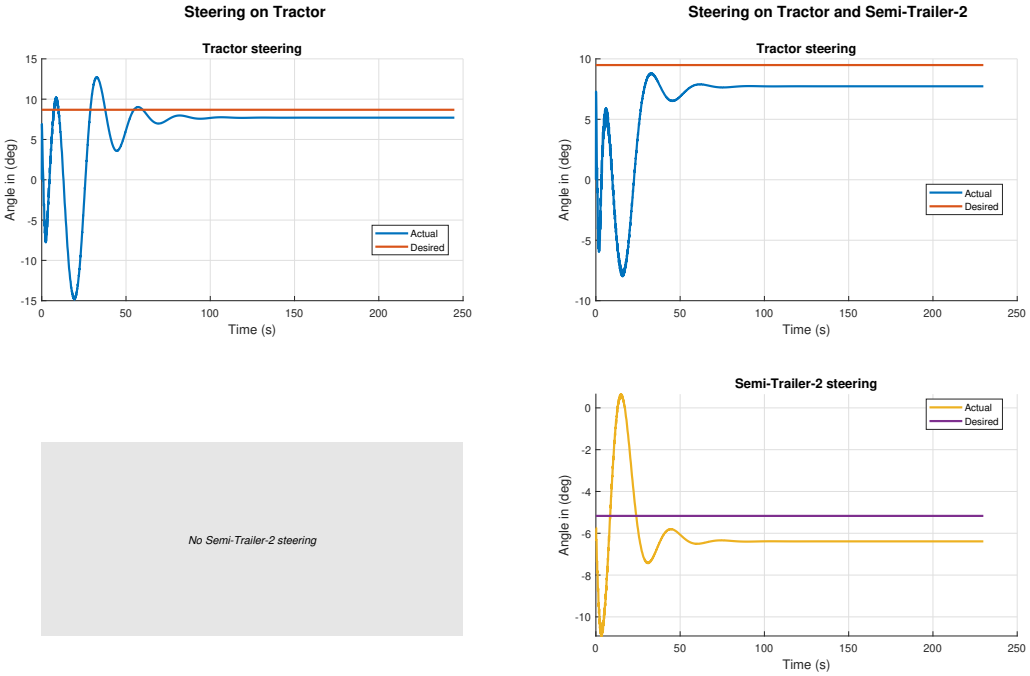

(a) Steering angle input

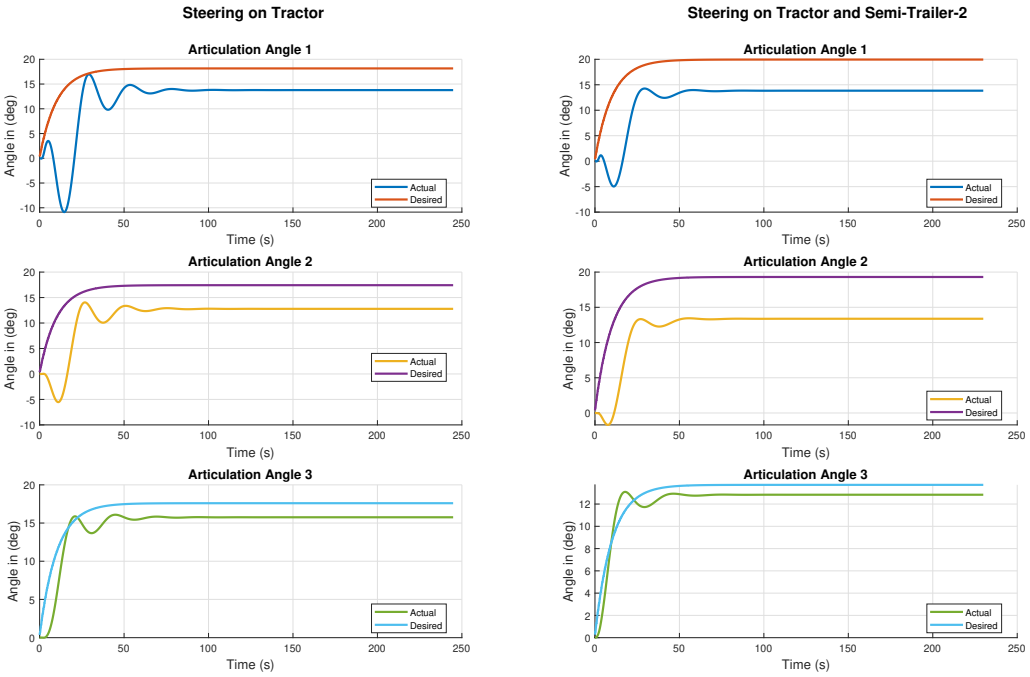

(b) Articulation angle output

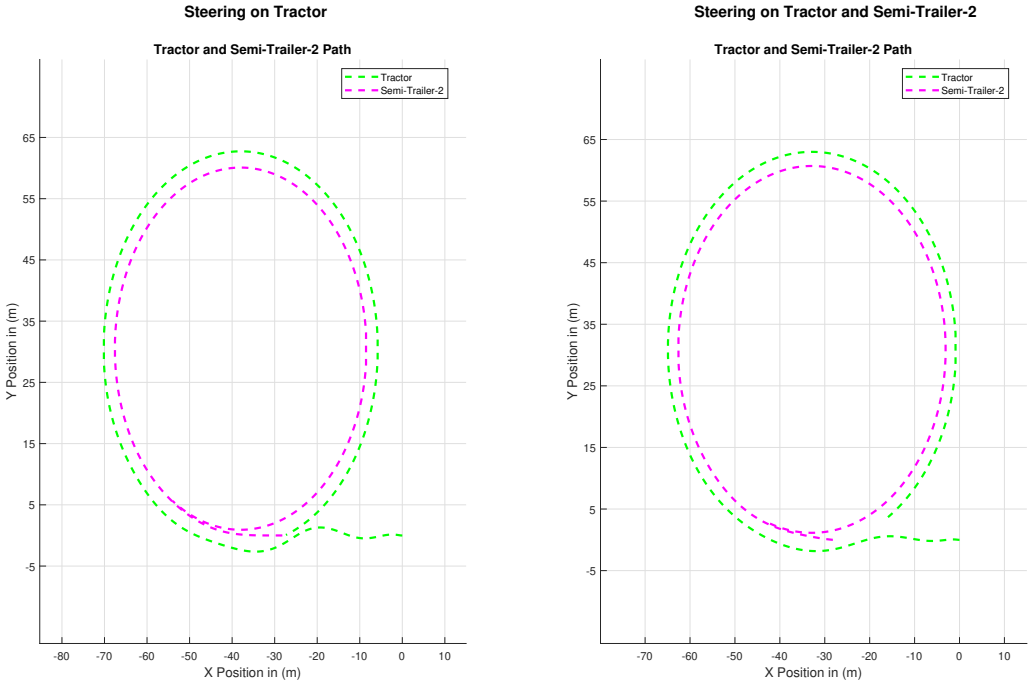

(c) Path of the Tractor and the Semi-trailer-2 while reversing

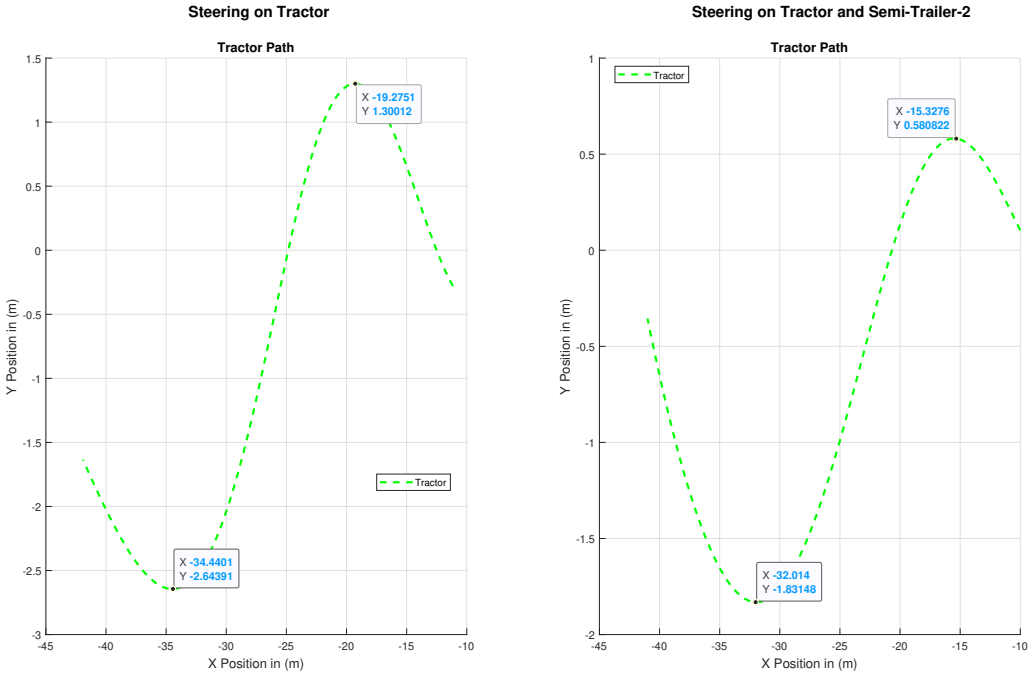

(d) Transient Swept Width of Tractor

Figure 4.3: Steering input, Articulation angle output, Path and Transient Swept width for test case 5 & 6

Performance metrics:

Table (4.1) shows Min-Max normalized performance metrics for a A-double reversing in a circle of 30m radius which is based on the Table (A.1) and the following can be deduced,

1. **Off-Tracking**: Off-tracking was lower when using both steering input. Among all the test cases, the test cases with all axle model seem to exhibit highest off-tracking when compared with the lumped axle model.

2. **TSC:** From the table it can be seen that, TSC is higher when both steering inputs were used. Similar to the off-tracking, the TSC in all axle model is higher than the lumped model.

3. **Quickness:** The vehicle completes its maneuver faster when using both steering inputs were used. All axle model with laden mass in the semi-trailer-1 is $3\% \sim 7\%$ quicker than the model with unladen semi-trailer-1.

4. **TSW:** TSW is lesser when both the steering inputs were used. From the data, it can be seen that the TSW is lesser when lumped model is used. In the all axle models TSW is lesser when using the model with unalden semi-trailer-1.

In all the performance metrices mentioned above the lumped model outperforms the all-axle model.

Test Case	**Off tracking**	**TSC**			**Quickness**	**TSW**
		TSC_1	TSC_2	TSC_{total}		
1	0.76	0.51	0.00	0.34	0.56	0.65
2	0.00	0.00	0.19	0.00	0.00	0.00
3	0.81	0.67	0.00	0.47	0.76	1.00
4	0.55	1.00	1.00	1.00	0.54	0.85
5	1.00	0.56	0.00	0.38	1.00	0.83
6	0.47	0.60	0.59	0.58	0.58	0.33

Table 4.1: Min-max normalized performance metrics for a circular path of radius 30 m

4.1.2 Straight line maneuver:

Test case 7 & 8:
In the test case 7 & 8, lumped was simulated in a 200m straight line maneuver. From the input responses shown in Fig. (4.4a) shows the steering input, where it can be observed that when only the tractor steering is used, the input is oscillatory with a peak-to-peak steering of 20° and the input settles around 90 seconds from the start of the transition to the straight line maneuver. Whereas when both steering inputs are used, the tractor steering input is smooth and reaches steady state at around 70

seconds from the start of the transition to the straight line maneuver. The steering input of the semi-trailer-2 approached steady state around 60 seconds from the start of the transition to the straight line maneuver. Similarly to the circular maneuver, the articulation angles follow the steering input, which can be seen in Fig. (4.4b).

Fig. (4.4c) shows the path made by the tractor and the semi-trailer-2. It can be seen that when two steering inputs are used, both tractor and semi-trailer-2 path is tracked without much of the off-tracking when compared with the tractor only steered case during the transition phase.

Test case 9 & 10:
In the test case 9 & 10, all axle was simulated in a 200m straight line maneuver. From the fig. (4.5a), it is evident that when all axle model is used, the input takes longer to reach steady state. The model with tractor only steered does not reach steady state with the 200m straight and has a peak-to-peak steering of 33°. The simulation might have to run for a longer period to see where the input settles. When both steering inputs were used, the input reaches steady state before the maneuver is complete. The peak-to-peak pattern observed is 19° for tractor steering, 9° for semi-trailer-2 steering, and both steering inputs converge in steady state at around 100 seconds. Similar behavior can be seen predominantly with articulation angles in Fig. (4.5b). With the test case 9, the articulation angle 1 exhibits a similar behavior as the steering input, whereas articulation angle 2 & 3 reaches steady state faster than the articulation angle 1. Whereas in test case 10, the articulation angle overshoots initially but then reaches steady state as time progresses.

As seen in Fig. (4.5c), tractor swing is observed in both test cases due to the overshoot in the steering input, the tractor then converges with the path when the steering input tries to converge to its steady state; nevertheless, when both steering inputs are used, it is decreased. In contrast to the lumped model, the tractor swing is apparent when utilizing the all axle model. This could be due to the inclusion of inter-axle impacts.

Test case 11 & 12:
All axle models with unladen mass on the semi-trailer-1 were simulated in a 200-meter straight line maneuver in test cases 11 and 12. As illustrated in Fig. (4.6a), the steering input converges to steady state before to the maneuver being completed, in contrast to the laden case with only a tractor steered. The controller generates a peak-to-peak steering input of 21°, which is $\sim$ 30% less than that of test case 9. When both steering inputs are applied, the peak-to-peak of the semi-trailer-2 is 9°, which is equivalent to the peak-to-peak observed in test case 10, and the tractor steering's is 14°, which is 26% less than the test case 10. Unlike test case 9, the articulation angle for test case 11 reaches steady state, which can be seen in Fig. (4.6b) steering converges to steady state.

When comparing the path shown in Fig. (4.6c) of the tractor and semi-trailer-2 to test cases 9 and 10, it is evident that the tractor swing is significantly less in both

of these test cases.

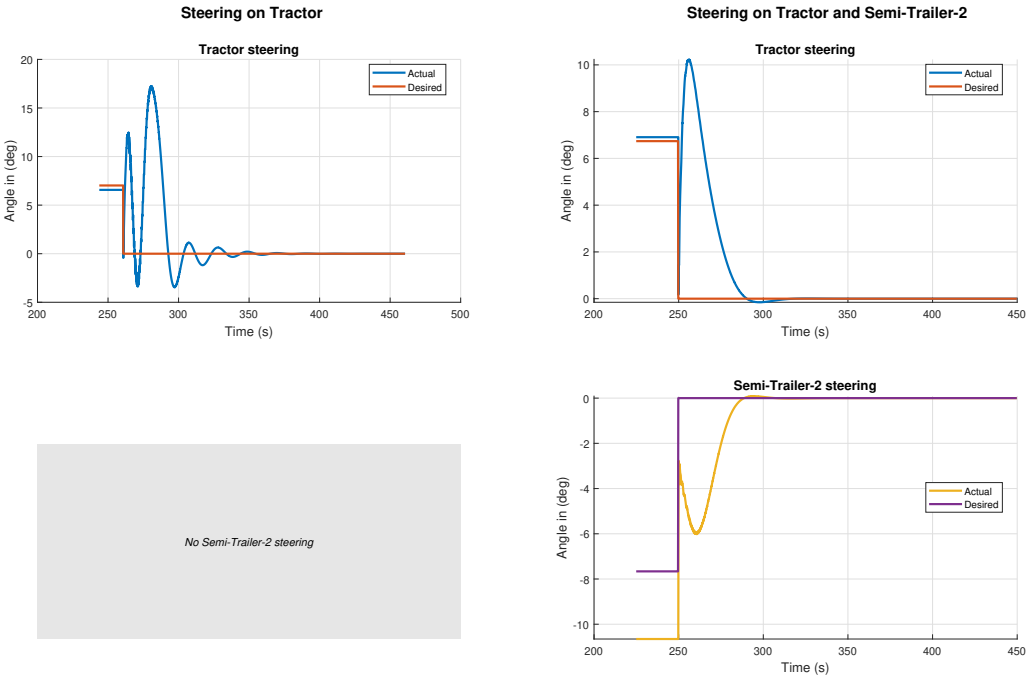

(a) Steering angle input

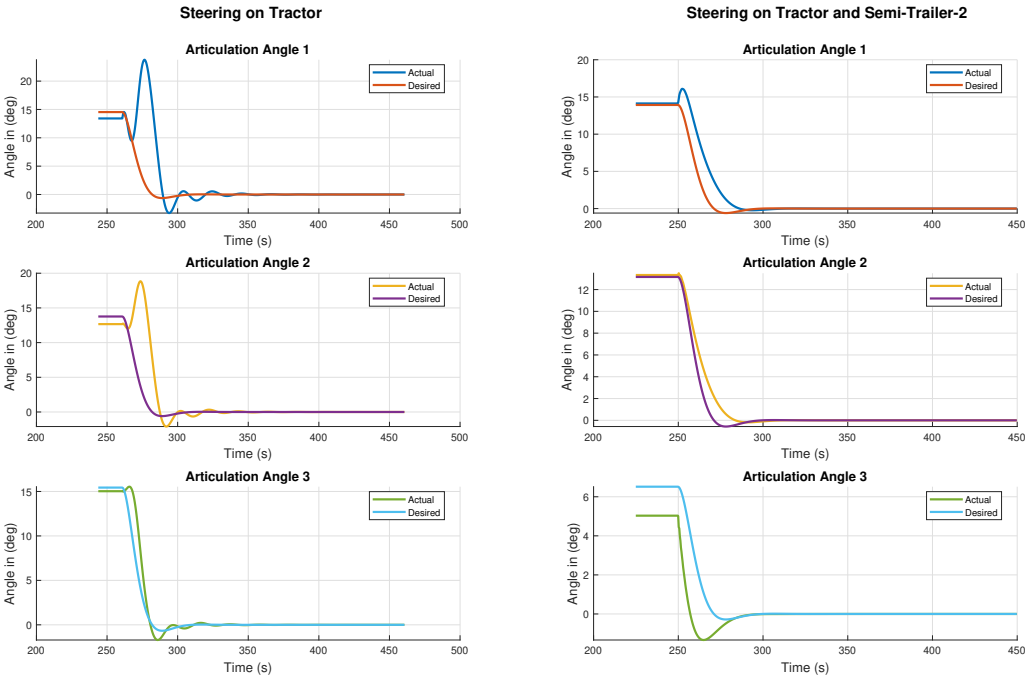

(b) Articulation angle output

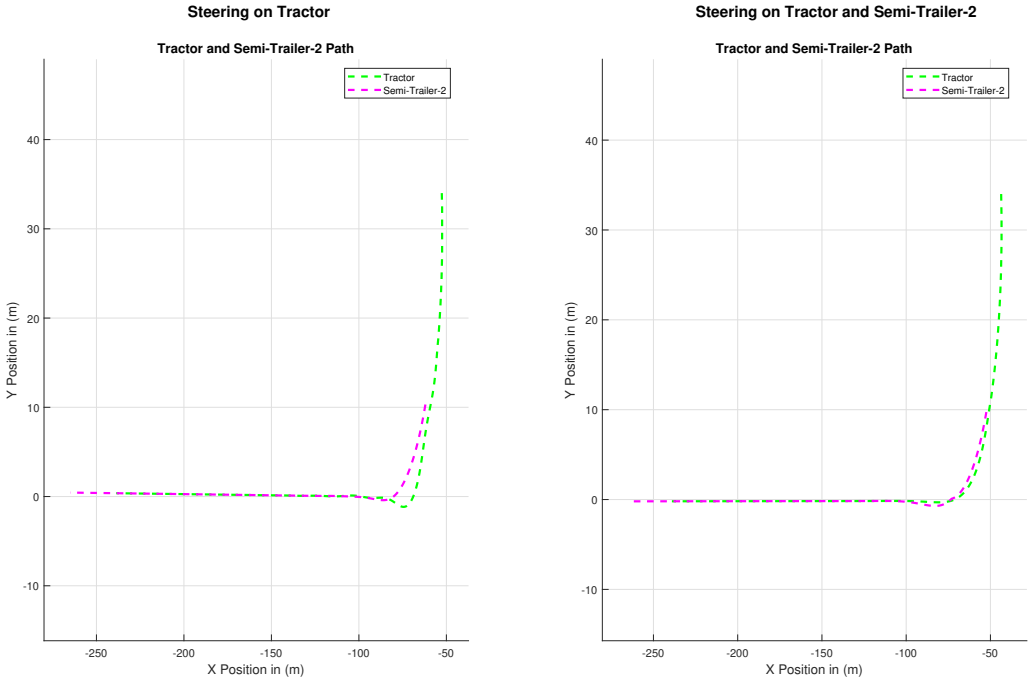

(c) Path of the Tractor and the Semi-trailer-2 while reversing

Figure 4.4: Steering input, Articulation angle output and Path for test case 7 & 8

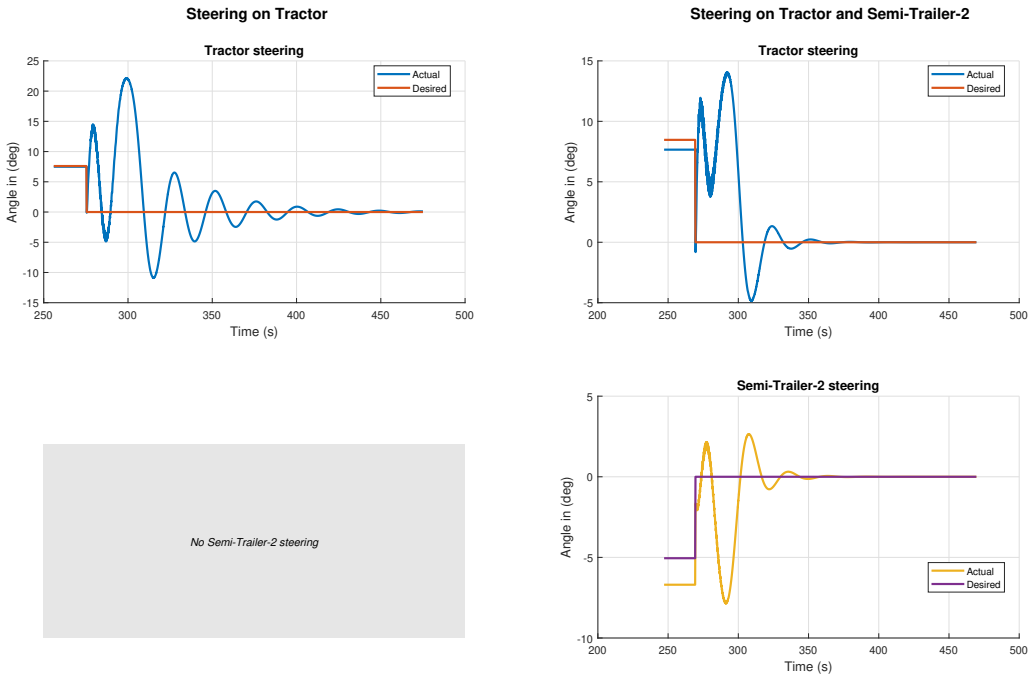

(a) Steering angle input

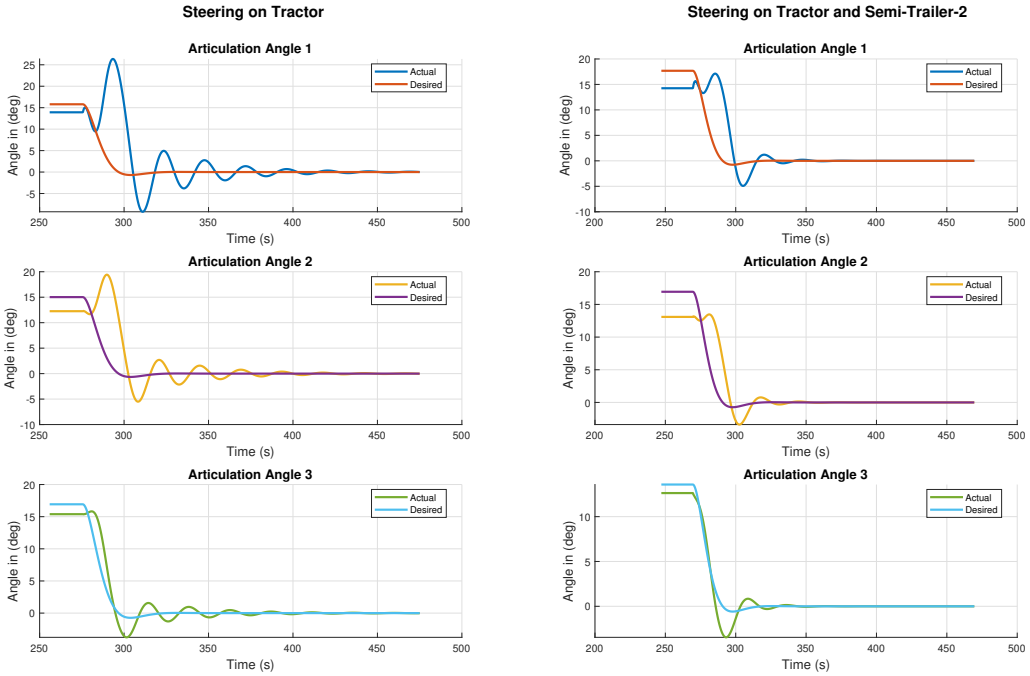

(b) Articulation angle output

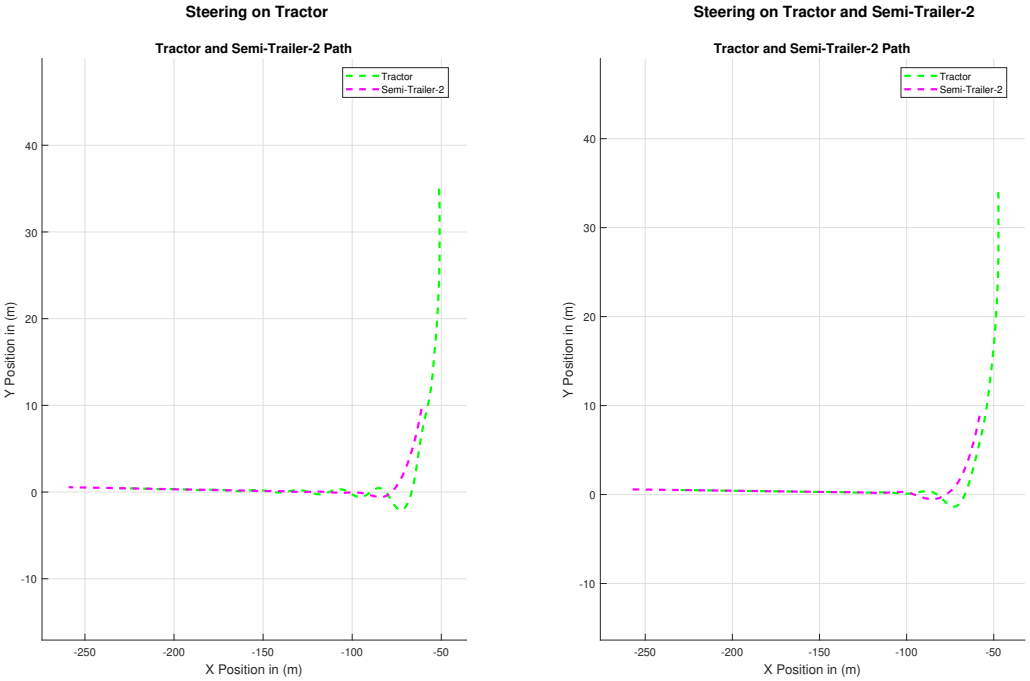

(c) Path of the Tractor and the Semi-trailer-2 while reversing

Figure 4.5: Steering input, Articulation angle output and Path for test case 9 & 10

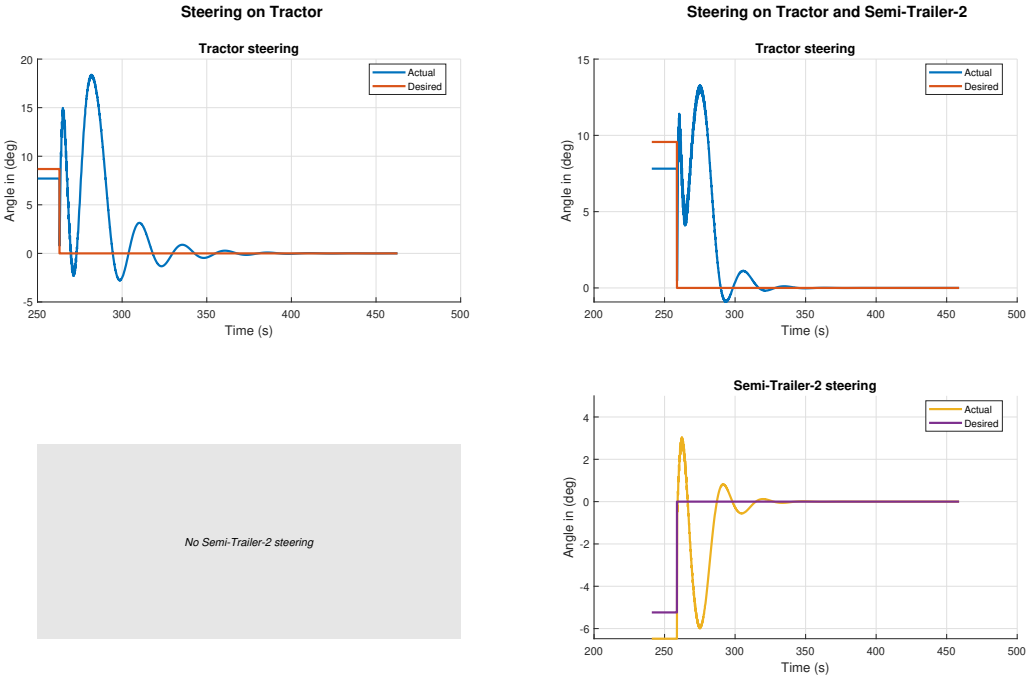

(a) Steering angle input

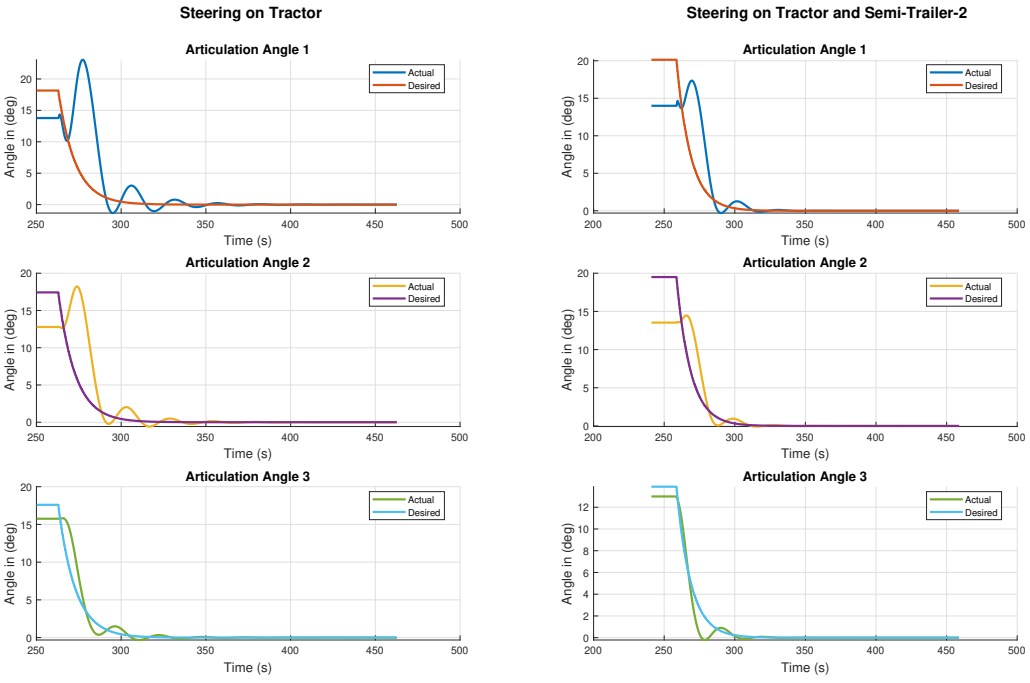

(b) Articulation angle output

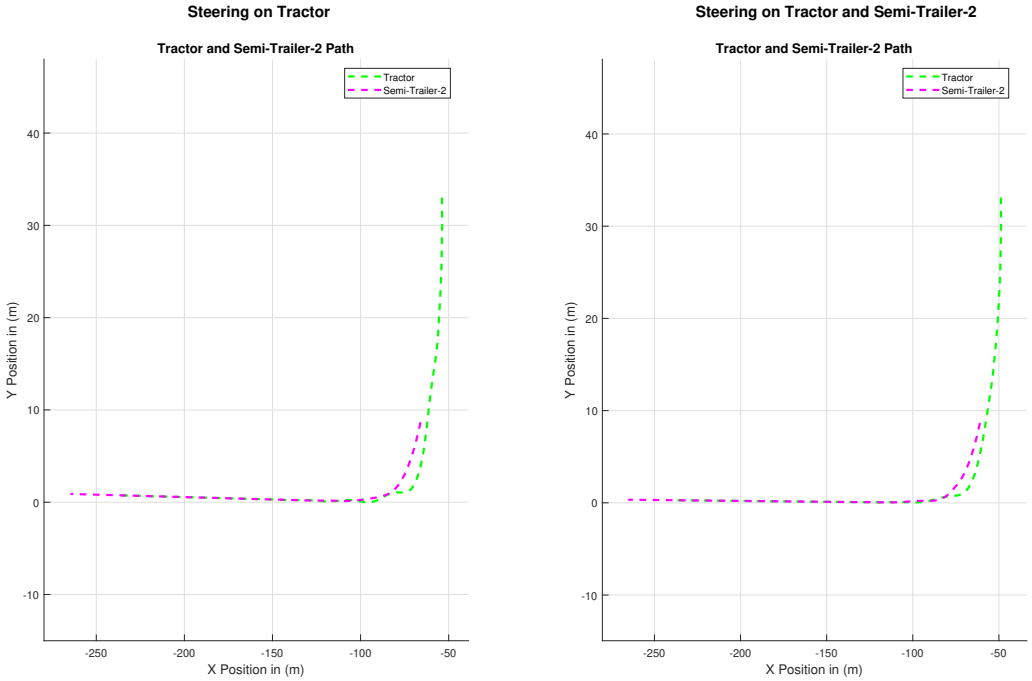

(c) Path of the Tractor and the Semi-trailer-2 while reversing

Figure 4.6: Steering input, Articulation angle output and Path for test case 11 & 12

Performance metrics:

Table (4.2) shows Min-Max normalized performance metrics for a A-double reversing in a straight line of length $200m$ based on Table (A.3) and the following can be deduced.

1. **Off-Tracking**: Off-tracking is lower in both the lumped models. In the all axle model, the off-tracking is minimal when having both the steering inputs.

2. **TSC:** Lumped model with two steerable inputs outperforms when compared with all the other test cases. In the all axle cases, the steering corrections are more when using two steering inputs similar to the circular maneuver.

Test Case	**Off tracking**		**TSC**		
	Steady state in curve	**Steady state in straight line**	TSC_1	TSC_2	TSC_{total}
7	0.00	0.00	0.71	0.00	0.49
8	0.27	0.00	0.00	0.21	0.00
9	0.73	1.00	1.00	0.00	0.72
10	0.87	0.001	0.97	0.63	0.98
11	0.91	0.029	0.69	0.00	0.47
12	1.00	0.001	0.79	1.00	1.00

Table 4.2: Min-max normalized performance metrics for a straight line maneuver

4.1.3 Combined maneuver:

All axle models with loaded semi-trailer-1 were simulated in a combined test scenario for test cases 13 and 14. It is evident from the steering input in Fig. (4.7a) that the input generated by the tractor's controller has a lower peak-to-peak when two steering inputs are used as compared to when only tractor steering is being used. But the peak-to-peak on the steering of the semi-trailer-2 is significantly higher when maneuver changes. In the case where two steering inputs are used, the controller reaches steady state faster. It can be observed from the steering plots that the desired steering angle for tractor and semi-trailer-2 are in opposite directions when negotiating curves. This is beneficial, especially when negotiating tight curves.

As seen in (4.7b), the articulation angles respond more smoothly when two steering inputs are applied. Compared to the test case where only tractor steering is utilized, the articulation angles attain a stable state more quickly. When only tractor steering was used, peak-to-peak articulation angles increased when the maneuver changed from straight line to the 90° curve. In both test case 13 & 14 articulation angle 2 & 3 have lower peak-to-peak value when compared to the arituclation angle 1, this could be due the delay between the units.

It is evident from the Fig. (4.7c) that the controller helps the truck to effectively maintain the path in both test case 13 & 14. When using two steering inputs, the tractor swing is significantly less when the maneuver changes.

Fig. (4.7d), shows the TSW when the maneuver changes from straight line reverse to the radius of 50 m. The TSW is 2.79 m when tractor is steered whereas it is 1.43 m when two steering inputs are used which is $\sim 47\%$ less.

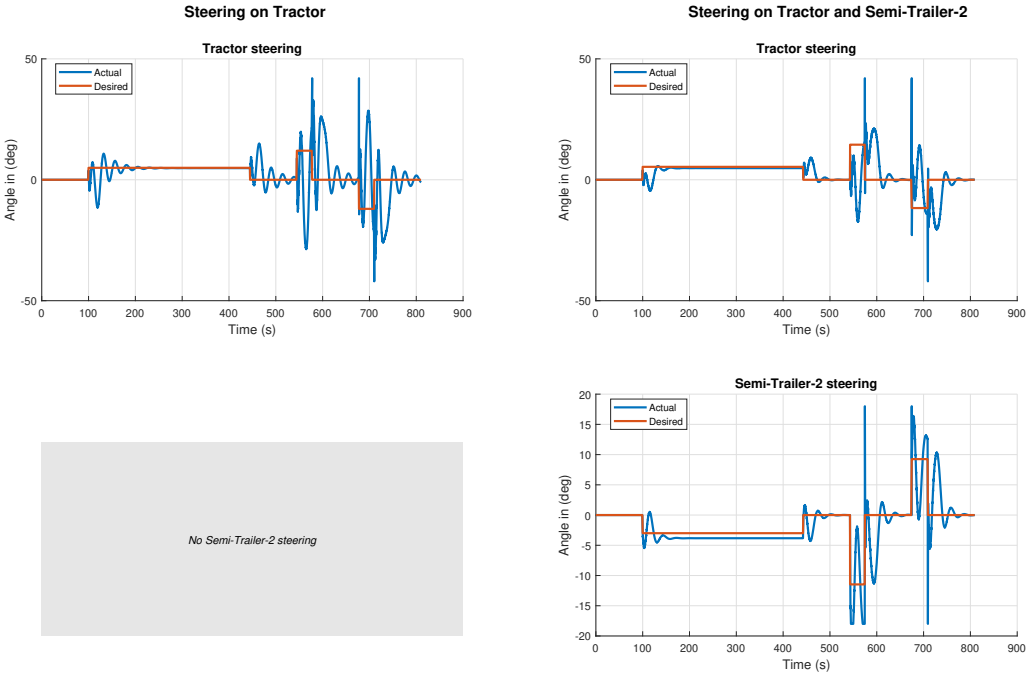

(a) Steering angle input

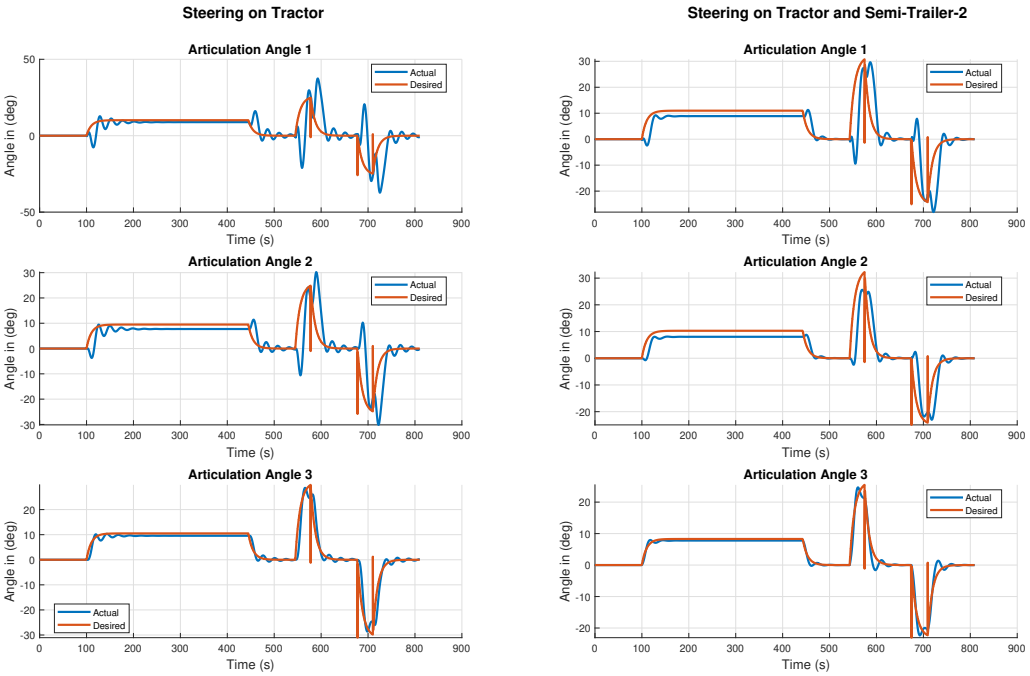

(b) Articulation angle output

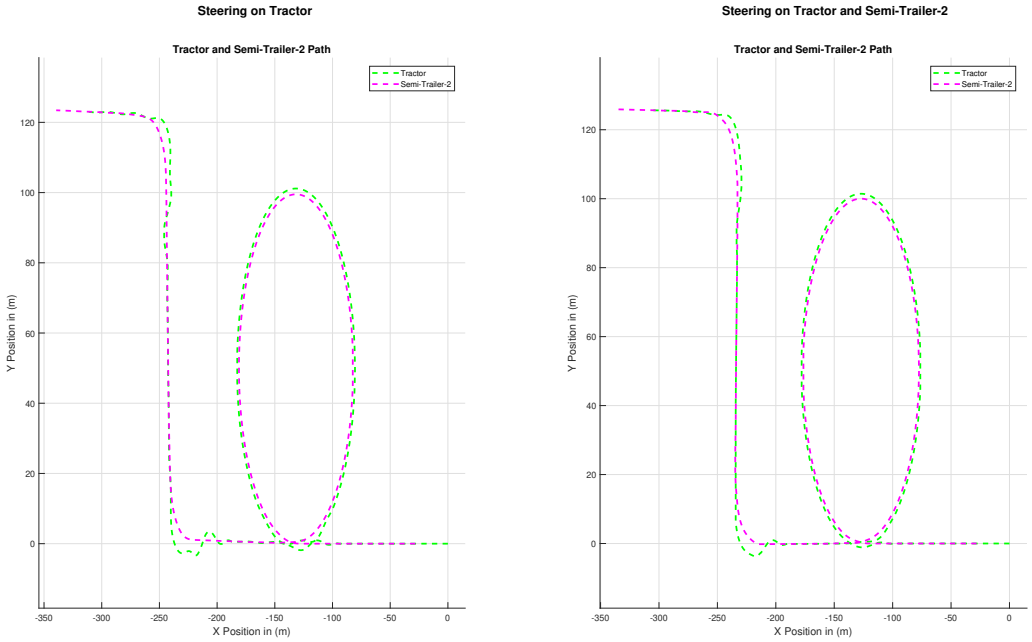

(c) Path of the Tractor and the Semi-trailer-2 while reversing

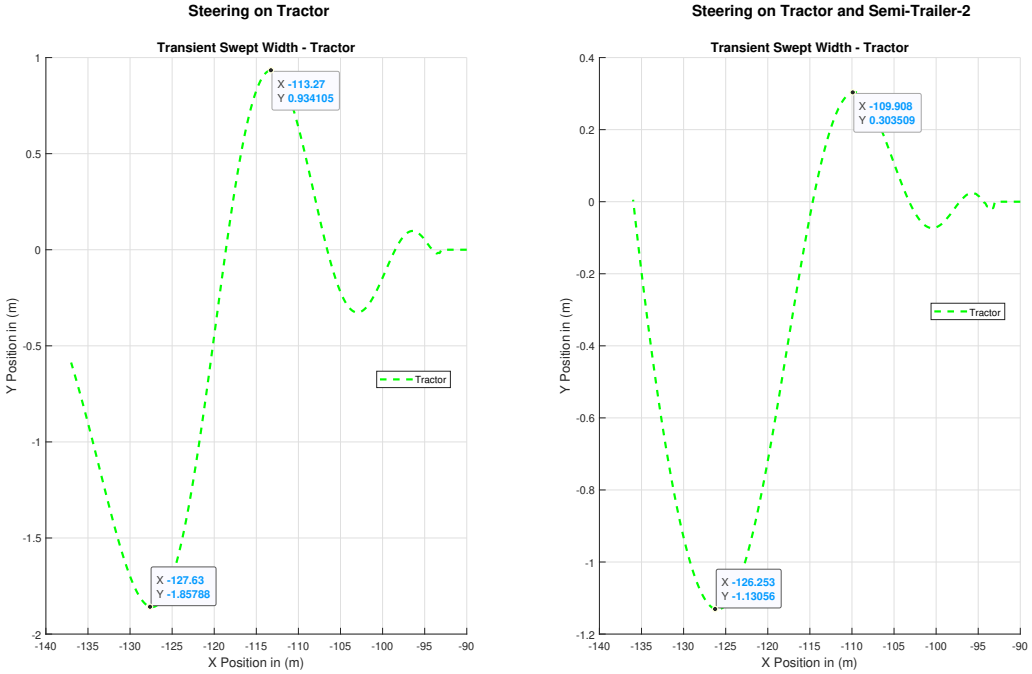

(d) Transient Swept Width of Tractor

Figure 4.7: Steering input, Articulation angle output, Path and Transient Swept width for test case 13 & 14

Performance metrics:

Table (4.3) presents Min-Max normalized performance metrics for a A-double reversing in a combined maneuver based on Table (A.5)

1. **TSC:** Number of steering corrections made is lesser when having only tractor steered.

2. **Quickness:** Similar to the circle maneuver, the vehicle is faster when using two steerable inputs.

3. **TSW:** TSW is lesser when using two steerable inputs which is similar to the circle maneuver.

Test Case	**TSC**			**Quickness**	**TSW**
	TSC_1	TSC_2	TSC_{total}		
13	0.00	0.00	0.00	1.00	1.00
14	1.00	1.00	1.00	0.00	0.00

Table 4.3: Min-max normalized performance metrics for a combined maneuver

5
Conclusion and Future Work

In this section, the goals presented in Section (1.3) are addressed and possible factors that could be included in future work are discussed.

5.1 Conclusion

The main objectives of this thesis were to investigate the benefits of employing two steerable axles and to design an effective controller to reverse an A-double combination at low speeds, which was achieved.

From the investigation carried out, it was understood that the reverse assist functionality of the trailer is used in passenger car segments, but not in trucking industry. However, trailer manufacturers have started looking into displaying the position of the vehicles on the display to reduce the risk of collision.

A real vehicle test was carried out with a driver with the intent to achieve this goal. The driver had to drive back and forth to reverse the A-double combination, because it was difficult to reverse for ten meters straight, according to the test data.

Both the tractor and the last axle of the semi-trailer-2 steered were taken into account when developing a proportional controller. Fourteen different test cases with three different maneuvers were simulated, and performance metrics were compared to see if adding the semi-trailer-2 would be beneficial. Overall, having steerable axles on the semi-trailer-2 with the tractor steering is beneficial as the off-tracking is lower, the truck takes the maneuver faster and the tractor swing is comparatively lesser than the single steering cases. Having only a tractor steered is beneficial in terms of total steering correction, which is lesser when compared to the cases having two steerable inputs, because when using two steering inputs, the controller tries to generate a steering angle to have lower off-tracking and lesser TSW, which helps in negotiating tight curves.

For the laden and unladen test cases, the combination that had unladen semi-trailer-1 performed better in both straight and circle maneuvers.

To achieve the HMI, a control knob and a display were set up in the simulation environment using Matlab Simulink based VTM model and Unreal engine, which worked as the intended design idea, with a realistic and user-friendly.

5.2 Future work

To potentially expand the research, the following could be considered.

1. The following can be included with the help of the force-based modeling approach.

   (a) Tire effects, including scrubbing, tire forces, and tire slip, etc. which helps in estimating the steering effort.

   (b) Predicting vehicle instability could be influenced by factors such as cornering stiffness, load transfers, inertia, and vehicle mass.

   (c) It is possible to study the behavior of low-grip surfaces and model the friction between the tire and the road.

2. Making proportional gains parametric is essential. As a result, it may not be necessary to adjust the gains when the vehicle combination or its specifications change.

3. A more sophisticated controller, such as an MPC, fuzzy logic controller, sliding-mode controller, etc., might be used.

4. Advanced control strategies can be developed by incorporating machine learning techniques such as reinforcement learning or neural network-based modeling.

5. Simulation was the basis in this research. Real-vehicle implementation of the controller suggested in this work is possible.

6. An appropriate steering rate limiter will have to be considered on the basis of the actuator dynamics.

7. A camera feed shall be used to show the environment to the driver.

8. In the HMI display, only the desired path is projected, but the actual path is not, the estimating the same would be beneficial, as it can be displayed to the driver.

9. A clinic with numerous test pilots could be done with the desktop simulation. Different curves can be tested in the HMI display.

10. Investigate the effect of having steering on other axles on the trailers, such as the dolly.

Bibliography

[1] Maliheh Sadeghi Kati. Definitions of performance based characteristics for long heavy vehicle combinations, 12 2013.

[2] Eurostat. Freight transport statistics - modal split, 2024.

[3] ACAE. New commercial vehicle registrations: vans +8.3

[4] Niklas Fröjd Lena Larsson, Emil Pettersson. Type vehicle combinations - hct sweden 25.25 to 34 meters. *HVTT forum*, 2015.

[5] Trans.INFO. Tsfs 2025:17, 2025. Accessed: 2025-04-16.

[6] Swedish Transport Agency. Swedish Transport Agency regulations on technical requirements for vehicle combinations exceeding 25.25 meters in length (TSFS 2023:42). `https://www.transportstyrelsen.se/globalassets/global/tsfs/2023/tsfs-2023-42.pdf`, August 2023. Decided on August 23, 2023. Entered into force on September 15, 2023. Repealed on April 15, 2025 by TSFS 2025:17.

[7] Trans.INFO. Sweden approves 34-metre-long vehicle combinations on national roads, 2025. Accessed: 2025-04-16.

[8] Road vehicles — Interchange of digital information on electrical connections between towing and towed vehicles — Part 3: Application layer, 2003.

[9] Thomas Edward Pilutti, Roger Arnold Trombley, Michael Hafner, Matthew Y. Rupp, Douglas Scott Rhode, and Darrel Alan Recker. TSFS 2025:17, 2014. Accessed: 2025-04-16.

[10] ZF. ZF Advanced Reversing Assist, 2020.

[11] Bosch. Trailer Tow Assist. Accessed: 2025-04-16.

[12] Nrupathunga Ashok, Vikram Parshetti, Lohith Reddy Keshava Reddy, Anand Prabhu, Pratham Jain, and Akhil Srinivas. Development of environments to test driver assist functions for reversing an a-double combination vehicle. Technical report, Chalmers University of Technology, 2021.

[13] Kouki Matsushita and Toshiyuki Murakami. Backward motion control for articulated vehicles with double trailers considering driver's input. In *IECON 2006 - 32nd Annual Conference on IEEE Industrial Electronics*, pages 3052–3057, 2006.

[14] Jesús Morales, Anthony Mandow, Jorge L. Martinez, Jorge L. Martínez, and Alfonso J. García-Cerezo. Driver assistance system for backward maneuvers in passive multi-trailer vehicles. In *2012 IEEE/RSJ International Conference on Intelligent Robots and Systems*, pages 4853–4858, 2012.

[15] Amy J. Rimmer and David Cebon. Implementation of reversing control on a doubly articulated vehicle. *Journal of Dynamic Systems, Measurement, and Control*, 139(6):061011, 04 2017.

[16] Zhaohui Ge, Fredrik Bruzelius, and Bengt Jacobson. Long combination vehicles reverse strategies based on articulation angle gradient. In Giampiero Mastinu, Francesco Braghin, Federico Cheli, Matteo Corno, and Sergio M. Savaresi, editors, *16th International Symposium on Advanced Vehicle Control*, pages 707–713, Cham, 2024. Springer Nature Switzerland.

[17] Niclas Evestedt, Oskar Ljungqvist, and Daniel Axehill. Path tracking and stabilization for a reversing general 2-trailer configuration using a cascaded control approach. In *2016 IEEE Intelligent Vehicles Symposium (IV)*, pages 1156–1161, 2016.

[18] A. Astolfi, P. Bolzern, and A. Locatelli. Path-tracking of a tractor-trailer vehicle along rectilinear and circular paths: a lyapunov-based approach. *IEEE Transactions on Robotics and Automation*, 20(1):154–160, 2004.

[19] C. Altafini, A. Speranzon, and B. Wahlberg. A feedback control scheme for reversing a truck and trailer vehicle. *IEEE Transactions on Robotics and Automation*, 17(6):915–922, 2001.

[20] Oskar Ljungqvist, Niclas Evestedt, Daniel Axehill, Marcello Cirillo, and Henrik Pettersson. A path planning and path-following control frameworkfor a general 2-trailer with a car-like tractor. *Journal of Field Robotics*, 2019.

[21] Adityen Sudhakaran. Autonomus paraller parking of a scaled tractor semitrailer, 2018.

[22] Krone Commercial Vehicle Group. Trailer axle drum brake – operating manual, n.d. Accessed: 2025-04-16.

[23] BPW Bergische Achsen KG. Steering axles workshop manual, 2017. Accessed: 2025-04-16.

[24] BPW Bergische Achsen KG. Active reverse control (arc) – electro-hydraulic auxiliary steering system for trailers, n.d. Accessed: 2025-04-16.

[25] VSE. Vse active steering system - product manual, n.d. Accessed: 2025-04-16.

[26] Jimmy Chiu and Ambarish Goswami. Driver assist for backing-up a vehicle with a long-wheelbase dual-axle trailer, 2014.

[27] A M C Odhams, R L Roebuck, and D Cebon. Implementation of active steering on a multiple trailer long combination vehicle.

[28] Roland Werner, Georg Kormann, and Steffen Mueller. Systematic model based path tracking control of actively steered implements in simulation and experiment. *IFAC Proceedings Volumes*, 46(18):85–90, 2013. 4th IFAC Conference on Modelling and Control in Agriculture, Horticulture and Post Harvest Industry.

[29] Xu Wang, Javad Taghia, and Jay Katupitiya. Robust model predictive control for path tracking of a tracked vehicle with a steerable trailer in the presence of slip. *IFAC-PapersOnLine*, 49(16):469–474, 2016. 5th IFAC Conference on Sensing, Control and Automation Technologies for Agriculture AGRICONTROL 2016.

[30] Road vehicles — Vehicle dynamics and road-holding ability — Vocabulary, 2011.

[31] Niklas Fröjd. Handling Analysis and Control Development of Commercial Trucks with Volvo Transport Models.

A

Appendix 1

A.1 Performance metrics

A.1.1 Circular Maneuver

Test Case	Off tracking (m)	TSC (rad)			Quickness (s)	TSW (m)
		TSC_1	TSC_2	TSC_{total}		
1	2.39	3.39	0.00	3.39	229.07	3.36
2	1.09	0.61	0.37	0.98	205.91	1.39
3	2.47	4.28	0.00	4.28	237.27	4.41
4	2.04	6.09	1.91	7.99	228.18	3.96
5	2.81	3.65	0.00	3.65	247.30	3.90
6	1.90	3.91	1.13	5.04	229.90	2.38

Table A.1: Performance metrics for a circular path of radius 30 m

Test Case	Off tracking	TSC_{total}	Quickness	TSW	Total Score
1	4	2	3	3	12
2	1	1	1	1	4
3	5	4	5	6	20
4	3	6	2	5	16
5	6	3	6	4	19
6	2	5	4	2	13

Table A.2: Ranking the performance metrics for a circular path of radius 30 m

A.1.2 Straight Maneuver

Test Case	Off tracking (m)		TSC (rad)		
	Steady state in curve	**Steady state in straight line (X 10^{-5})**	TSC_1	TSC_2	TSC_{total}
7	2.35	2.55	3.65	0.00	3.65
8	2.48	3.72	0.52	0.50	1.03
9	2.72	3531.10	4.94	0.00	4.94
10	2.79	6.75	4.80	1.53	6.33
11	2.80	103.12	3.57	0.00	3.57
12	2.85	5.12	4.00	2.43	6.44

Table A.3: Performance metrics for a straight line maneuver

Test Case	Off tracking in straight line	TSC_{total}	Total Score
7	1	3	4
8	2	1	3
9	6	4	10
10	4	5	9
11	5	2	7
12	3	6	9

Table A.4: Ranking the performance metrics for a straight line

A.1.3 Combined Maneuver

Test Case	TSC (rad)			Quickness (s)	TSW (m)
	TSC_1	TSC_2	TSC_{total}		
13	35.69	0.00	35.69	810.40	2.79
14	37.28	11.40	48.68	808.27	1.43

Table A.5: Performance metrics for a combined maneuver

Test case	Total TSC	Quickness	TSW	Total Score
13	1	2	2	5
14	2	1	1	4

Table A.6: Ranking the performance metrics for a combined maneuver

A.2 Plots for the performance metrics

A.2.1 Circle Maneuver

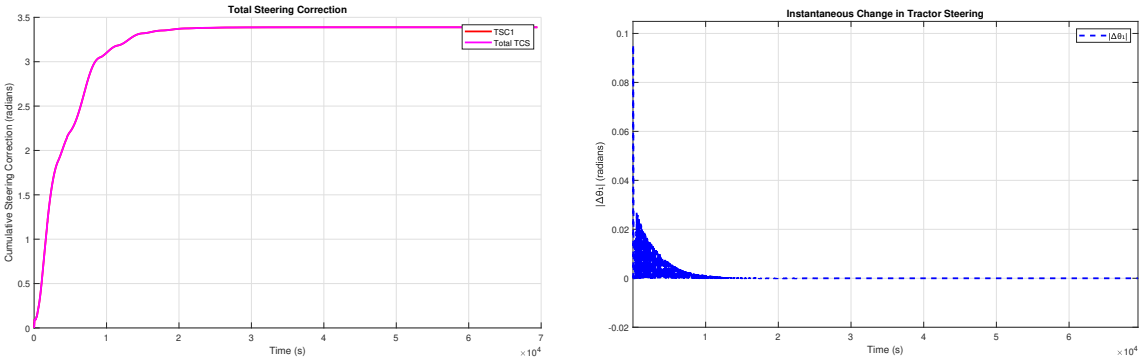

Figure A.1: TSC & Instantaneous change in steering - Lumped model - Tractor steering

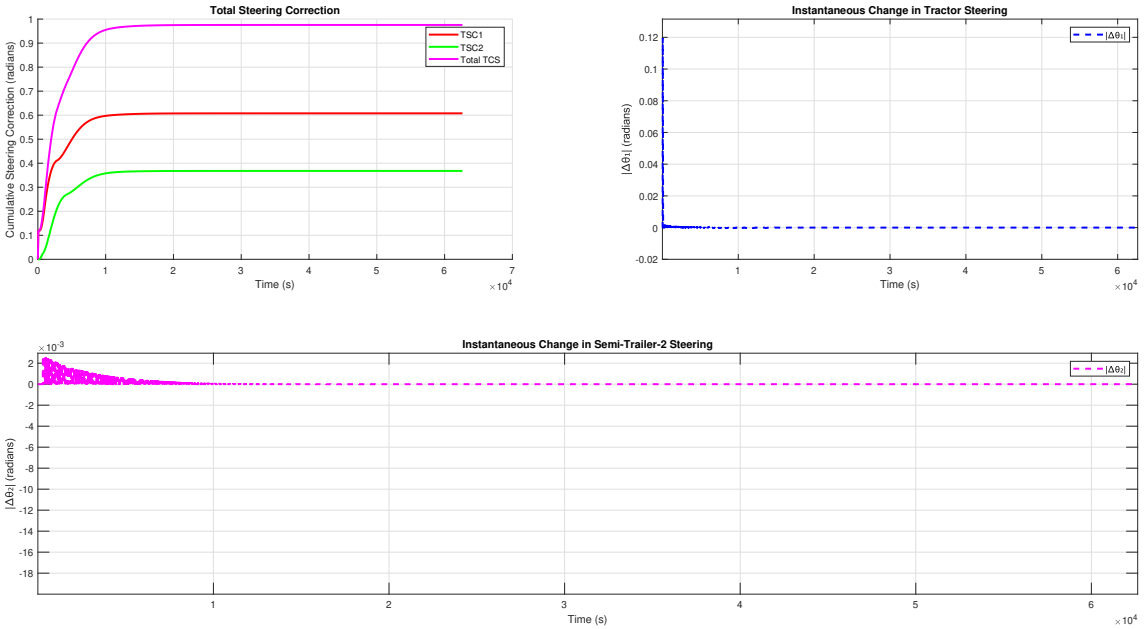

Figure A.2: TSC & Instantaneous change in steering - Lumped model - Tractor & Semi-trailer-2 steering

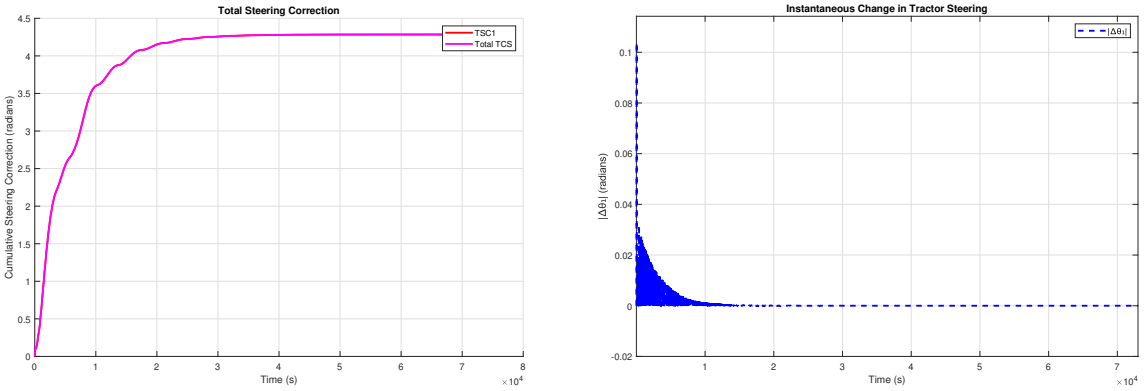

Figure A.3: TSC & Instantaneous change in steering - All axle model - Tractor steering

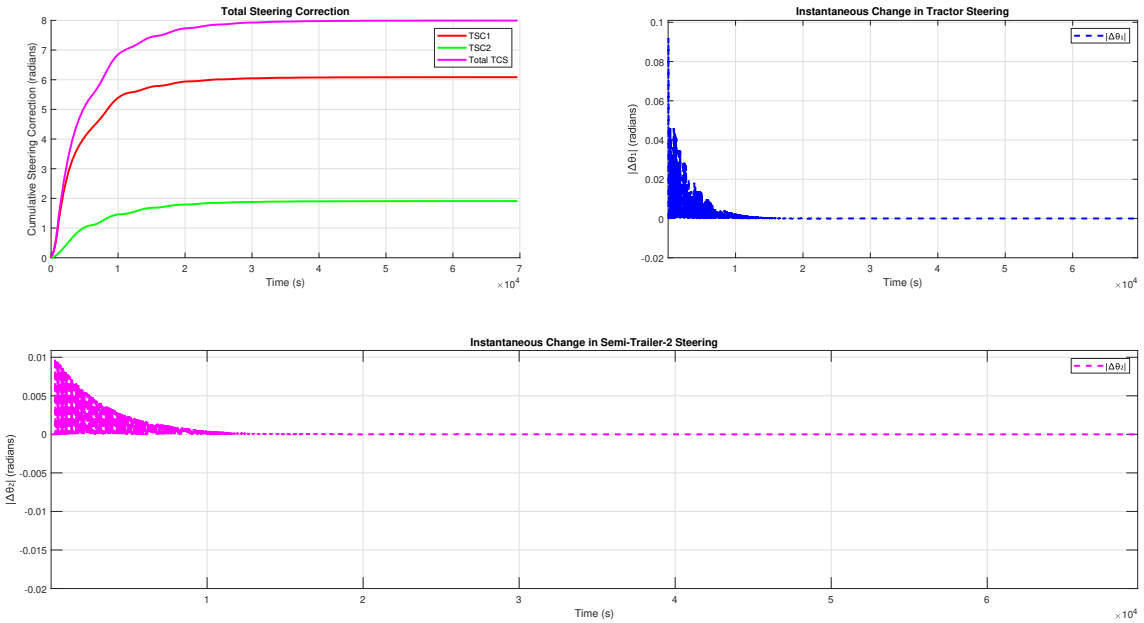

Figure A.4: TSC & Instantaneous change in steering - All axle model - Tractor & Semi-trailer-2 steering

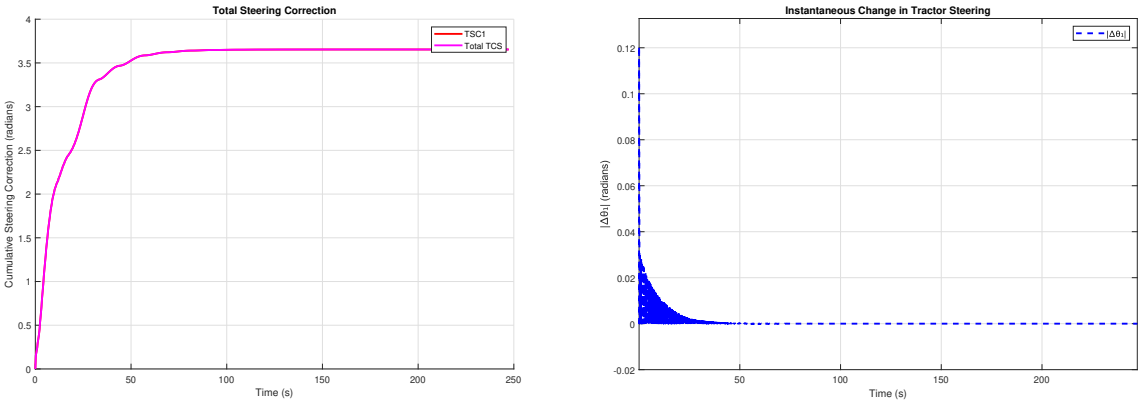

Figure A.5: TSC & Instantaneous change in steering - All axle model (unladen) - Tractor steering

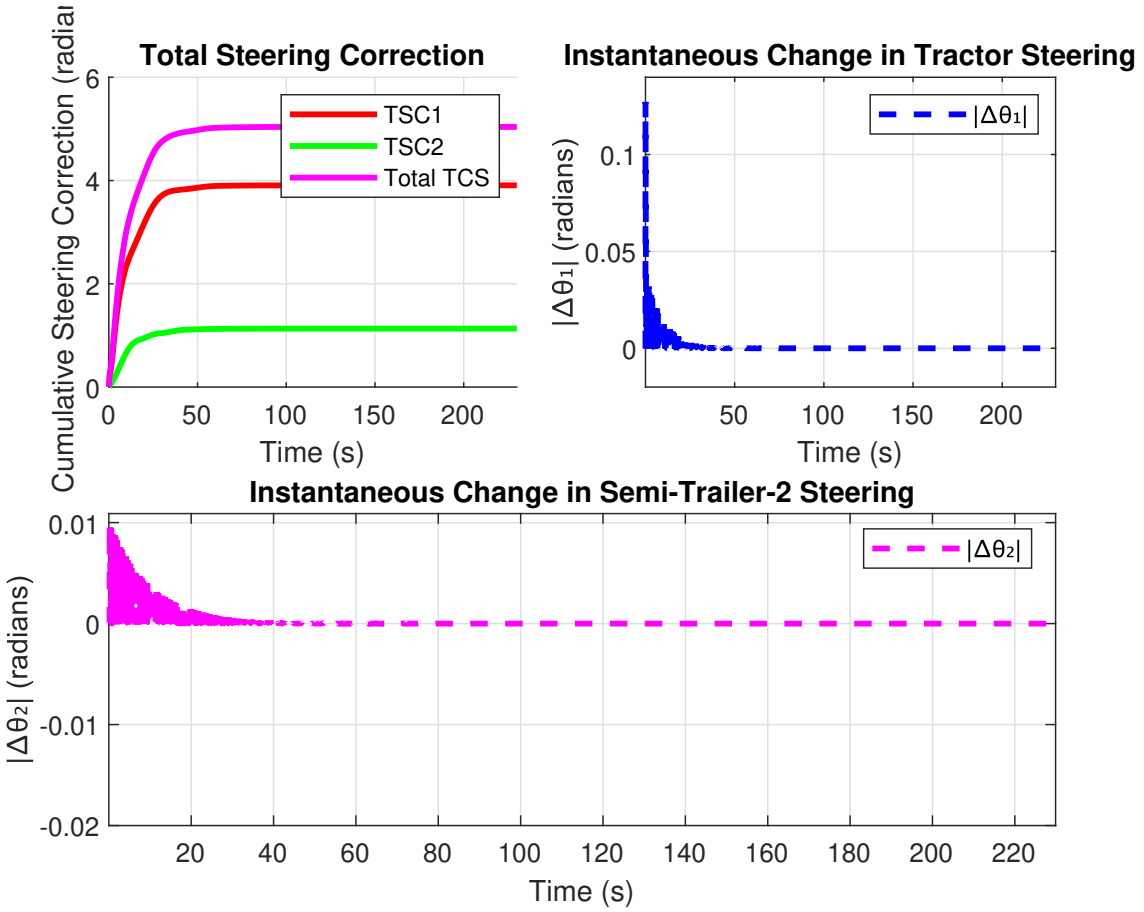

Figure A.6: TSC & Instantaneous change in steering - All axle model (unladen) - Tractor & Semi-trailer-2 steering

A.2.2 Straight Maneuver

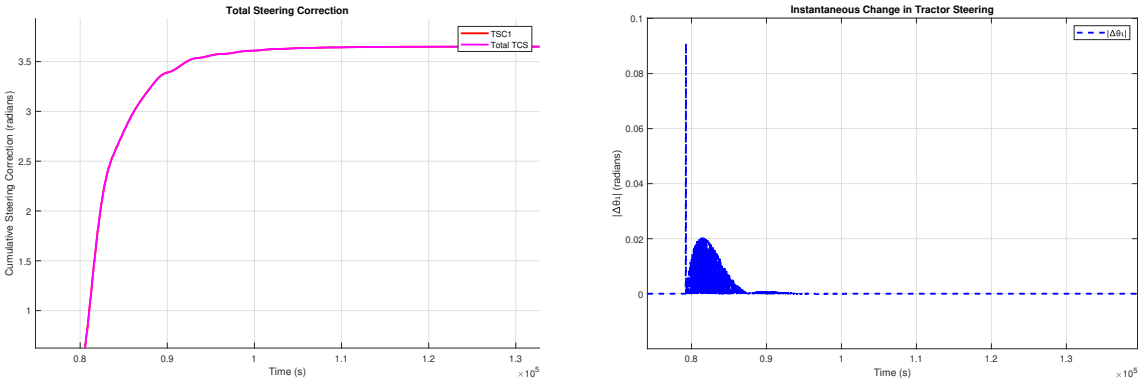

Figure A.7: TSC & Instantaneous change in steering - Lumped model - Tractor steering

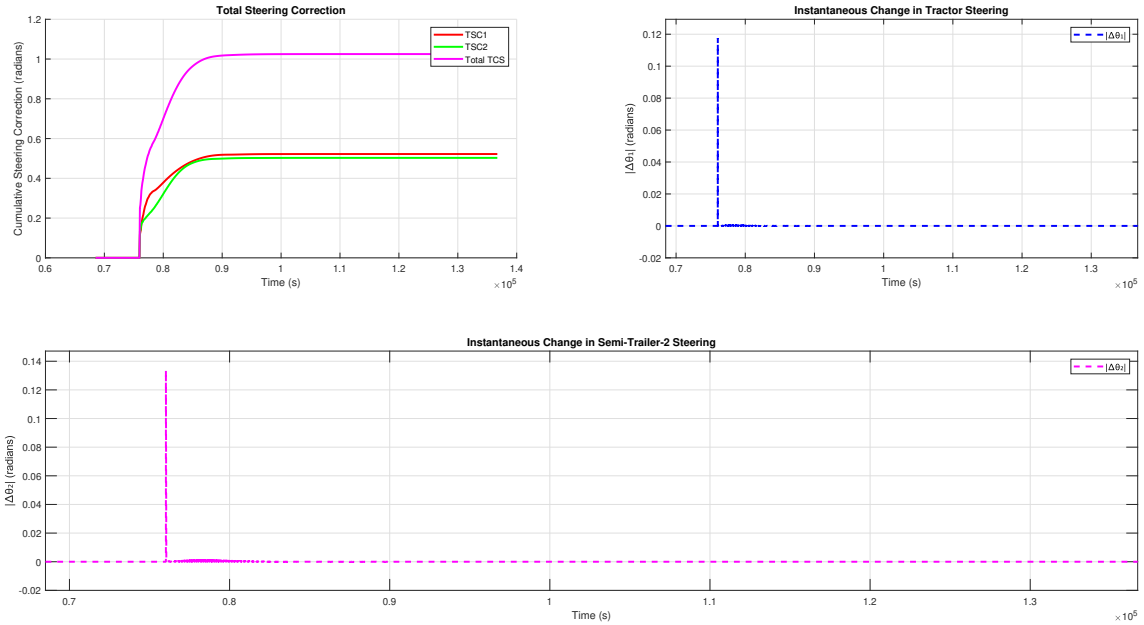

Figure A.8: TSC & Instantaneous change in steering - Lumped model - Tractor & Semi-trailer-2 steering

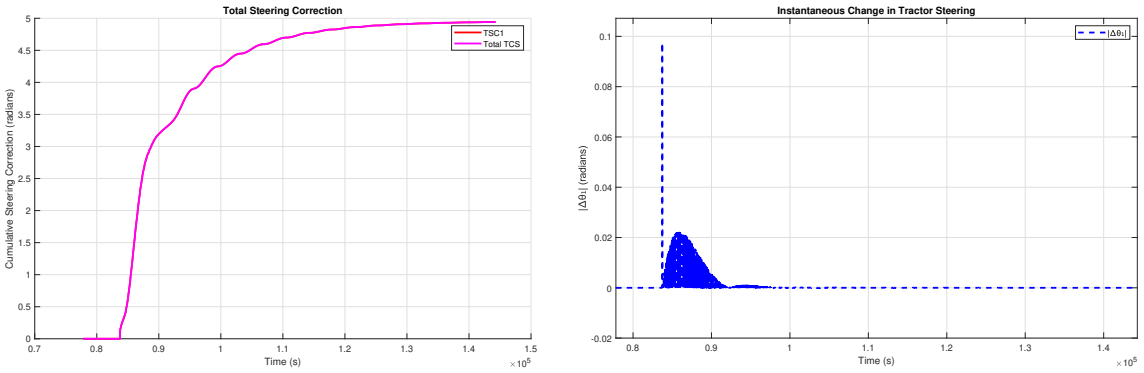

Figure A.9: TSC & Instantaneous change in steering - All axle model - Tractor steering

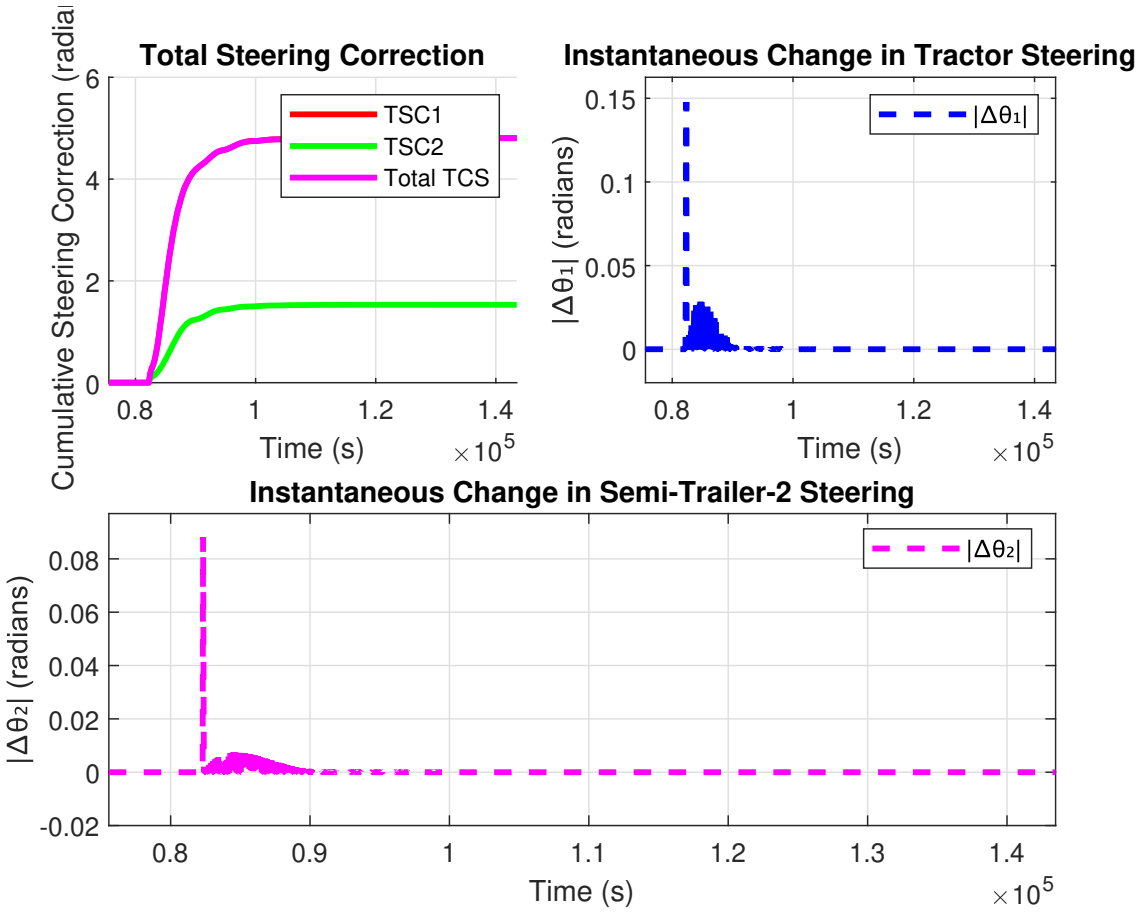

Figure A.10: TSC & Instantaneous change in steering - All axle model - Tractor & Semi-trailer-2 steering

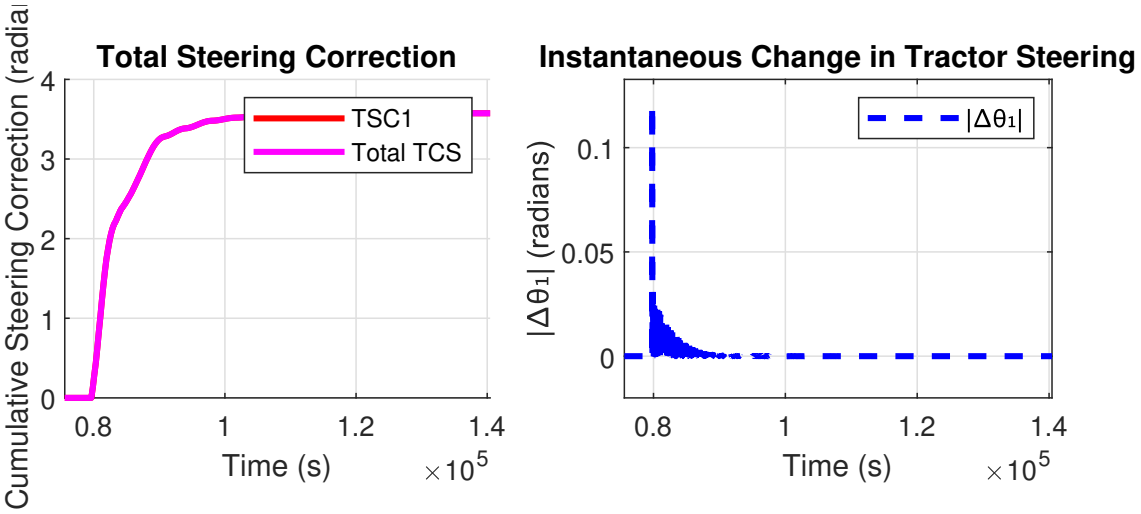

Figure A.11: TSC & Instantaneous change in steering - All axle model (unladen) - Tractor steering

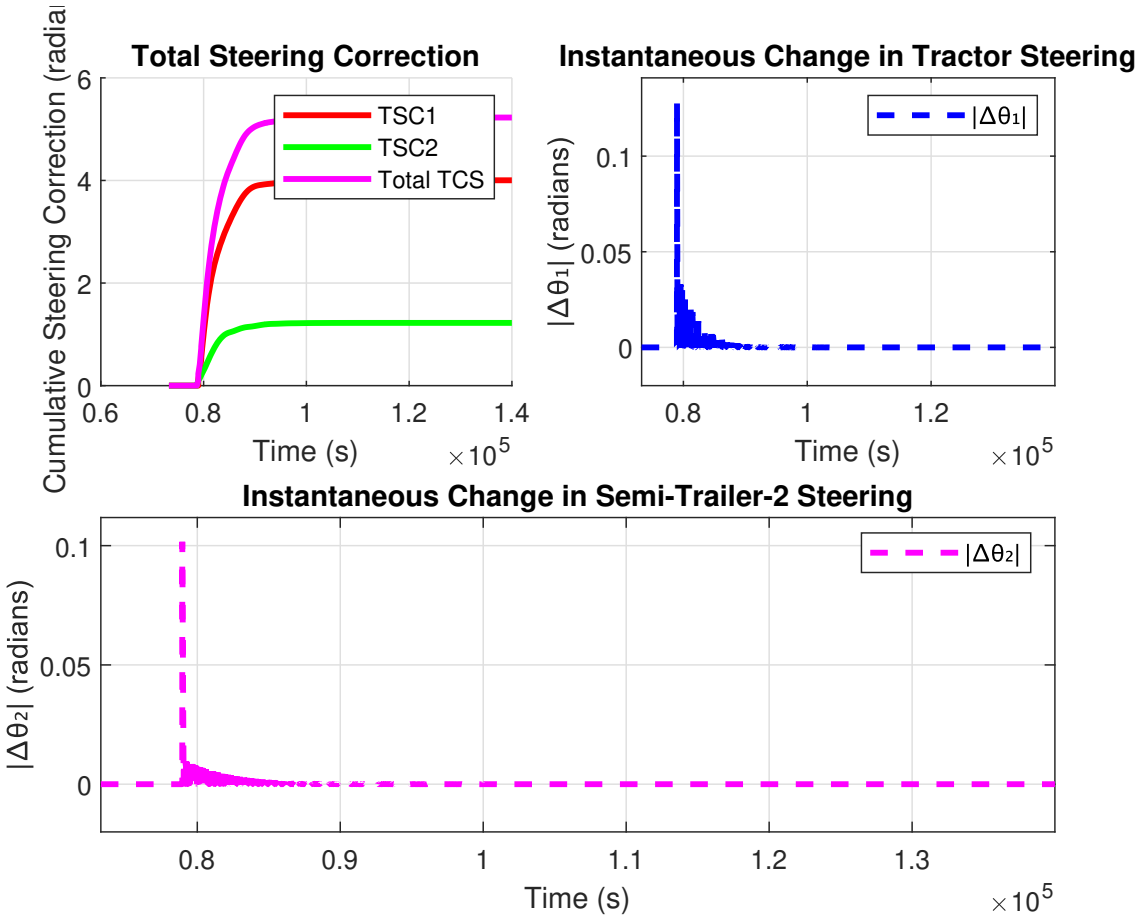

Figure A.12: TSC & Instantaneous change in steering - All axle model (unladen) - Tractor & Semi-trailer-2 steering

A.2.3 Combined Maneuver

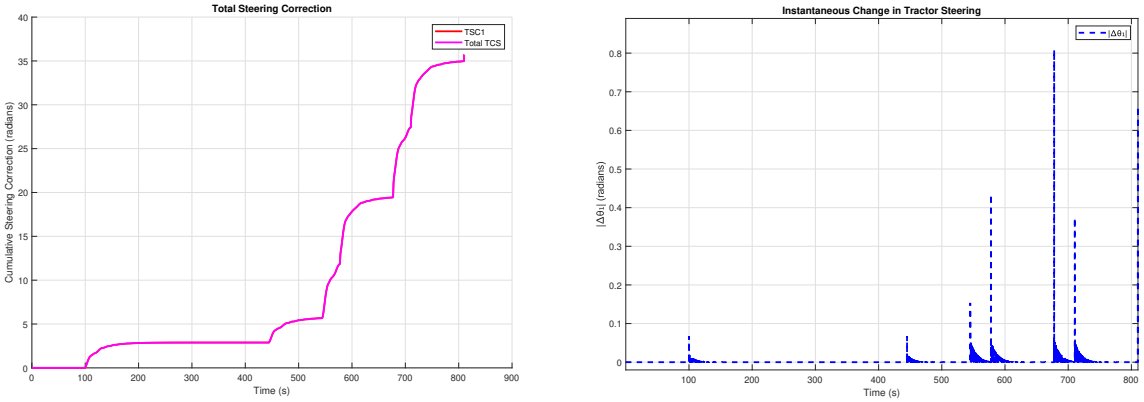

Figure A.13: TSC & Instantaneous change in steering - All axle model - Tractor steering

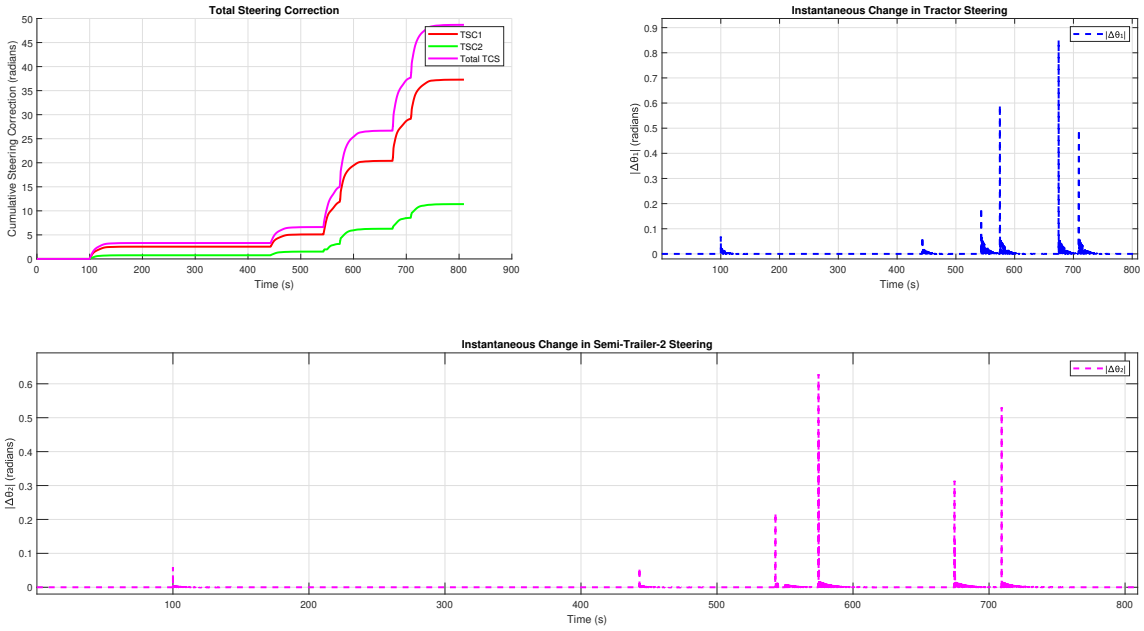

Figure A.14: TSC & Instantaneous change in steering - All axle model - Tractor & Semi-trailer-2 steering

DEPARTMENT OF MECHANICS AND MARITIME SCIENCES
CHALMERS UNIVERSITY OF TECHNOLOGY
Gothenburg, Sweden 2025
www.chalmers.se

CHALMERS
UNIVERSITY OF TECHNOLOGY